Earth-Science Reviews 226 (2022) 103926

Contents lists available at ScienceDirect

Earth-Science Reviews

journal homepage: www.elsevier.com/locate/earscirev

# Glacier change in China over past decades: Spatiotemporal patterns and influencing factors

Bo Su[a,b], Cunde Xiao[a,*], Deliang Chen[b,*], Yi Huang[a], Yanjun Che[c], Hongyu Zhao[a], Mingbo Zou[a], Rong Guo[d,e], Xuejia Wang[b,f], Xin Li[d], Wanqin Guo[g], Shiyin Liu[h], Tandong Yao[d]

[a] State Key Laboratory of Earth Surface Processes and Resource Ecology, Beijing Normal University, Beijing 100875, China
[b] Regional Climate Group, Department of Earth Sciences, University of Gothenburg, Gothenburg 40530, Sweden
[c] Department of Geography Science, Yichun University, Yichun 336000, Jiangxi, China
[d] State Key Laboratory of Tibetan Plateau Earth System, Resources and Environment (TPESRE), Institute of Tibetan Plateau Research, Chinese Academy of Sciences, Beijing 100101, China
[e] University of Chinese Academy of Sciences, Beijing 100049, China
[f] Key Laboratory of Western China's Environmental Systems (Ministry of Education), College of Earth and Environmental Sciences, Lanzhou University, Lanzhou 730030, China
[g] State Key Laboratory of Cryospheric Science, Northwest Institute of Eco-Environment and Resources, Chinese Academy of Sciences, Lanzhou 730000, China
[h] Yunnan Key Laboratory of International Rivers and Transboundary Eco-Security, Yunnan University, Kunming, Yunnan 650091, China

ARTICLE INFO

*Keywords:*
Glacier change
Influencing factor
Climate change
Chinese Glacier Inventories
China

ABSTRACT

China has the largest area of glaciers situated within the middle- and low-latitude areas worldwide. Rapid changes in mountain glaciers across western China in the last decades have not only affected glacial runoff and hazards but also had profound impacts on ecosystems and socioeconomic activities in the extensive cold and arid regions of Asia and even beyond. Therefore, research on glacier change is of significant importance for regional sustainability. This study re-analyzes the first and second Chinese Glacier Inventories (CGI-1 and CGI-2) and summarizes available in-situ observation-based studies on glacier mass balance and length to provide a spatially explicit and coherent national-scale assessment of glacier changes and associated influencing factors in recent decades. We connect the glaciers between CGI-1 (from the 1950s to the 1980s) and CGI-2 (from the 2000s to the 2010s) one by one to explore the area, volume, and Equilibrium Line Altitude (ELA) changes at both the individual glacier and river basin scales for the first time. The results show that the long-term area and volume changes in China's glaciers during the area-weighted average period from CGI-1 (around 1969) to CGI-2 (around 2008) were − 5.6%/decade and − 5.3%/decade, respectively, with a mean ELA change of 12.5 m/decade. Approximately 17.2% of the total number of glaciers in CGI-1 disappeared, only 5.5% of the glaciers advanced, and the majority of glaciers decreased in size during the period between CGI-1 and CGI-2, which was characterized by a shrinkage in area and volume and a rise in ELA or division into multiple branches. In-situ observation-based analysis shows that glacier length has reduced since at least the 1960s on average, and their trends have accelerated since the 1990s. The negative trend of mass balance was slightly larger than that of the reference glaciers globally during 1960–2019, while the mean mass loss in any given decade was lower than that of the global mean. The changes have different regional characteristics. Overall, the shrinkage increased from the interior to the southeast in the Tibetan Plateau and decreased from the northeast to the southwest in northern Xinjiang, including the Chinese Tien Shan Mountains. Climatic conditions, as reflected in annual mean temperature and precipitation, are the primary causes of different spatiotemporal patterns of glacier change. A significant positive correlation is observed between annual absolute area/volume changes and snowfall variations, and a significant negative correlation is found with rainfall variations, but there is no significant correlation between the indicators of air temperature and glacial changes at the river basin scale. Additionally, other local-scale factors, such as glacial morphology and topographic conditions, have exerted profound impacts on glacier retreat for individual glaciers.

* Corresponding authors.
*E-mail addresses:* cdxiao@bnu.edu.cn (C. Xiao), deliang@gvc.gu.se (D. Chen).

https://doi.org/10.1016/j.earscirev.2022.103926
Received 19 April 2021; Received in revised form 30 December 2021; Accepted 9 January 2022
Available online 14 January 2022
0012-8252/

## 1. Introduction

Mountain glaciers are a key part of Earth's cryosphere, and they can be highly sensitive to even small climatic fluctuations (Oerlemans, 2005; IPCC, 2013; IPCC, 2019). In recent decades, climate warming has accelerated and led to a widespread shrinking of glaciers globally, which not only affects river runoff, mountain hazards and global sea level but also has potentially severe implications for regional ecosystems, socio-economic activities, and human cultural and spiritual aspects (Haeberli and Weingartner, 2020; IPCC, 2013; IPCC, 2019; Milner et al., 2017; Zemp et al., 2015; Su et al., 2019; Zemp et al., 2019; Nie et al., 2021; Azam et al., 2021). Consequently, research on glacier changes, which include mechanisms, impacts, and adaptations, is a global concern and has received increasing attention (Qin et al., 2018; Su et al., 2019).

China has the largest number of glaciers across the middle- and low-latitude areas worldwide (Li et al., 2008; Shi et al., 2009). Recent studies have shown that there are a total of 48,571 glaciers with an area of approximately 51,840.1 km$^2$ (Guo et al., 2015; Liu et al., 2015), which account for 22.5% of the number and 7.3% of the area of glaciers globally in the up-to-date Randolph Glacier Inventory (RGI 6.0; 215,547 glaciers with a total area of 705,738.8 km$^2$) (Pfeffer et al., 2014). Glaciers in China are mainly distributed in the high mountains of the western region (49°09′-27°06′N, 103°54′- 71°32′E). Except for the Altai, Saur, and Tien Shan Mountains, which are located in the northern Xinjiang Uygur Autonomous Region of China, the others are concentrated on the Tibetan Plateau (TP), which is the "Third Pole of the Earth" and "Water Tower of Asia" (Immerzeel et al., 2010; Zhang et al., 2020) (Fig. 1-A). Approximately 248.2 million people (2015) depend in part on glacial meltwater in China (Su et al., 2022). Especially in northwestern arid inland basins with high water stress, including the Tarim, Junggar, Turpan-Hami, and Qaidam basins and Hexi Corridor, meltwater from glaciers in the Tien Shan, Qilian, and the northern Kunlun Mountains plays an extremely important role in the formation and development of local socioecological systems (Chen et al., 2015; Su et al., 2019). In addition, the glaciers on the Chinese TP and the Altai, and western Chinese Tien Shan Mountains also supply drainage runoff for many large international river basins with highly dense populations, such as the Brahmaputra, Ganges, Indus, Ob, Lake Balkash, Mekong, and Salween River basins (Bolch, 2017; Pritchard, 2019).

In recent decades, numerous studies have investigated China's

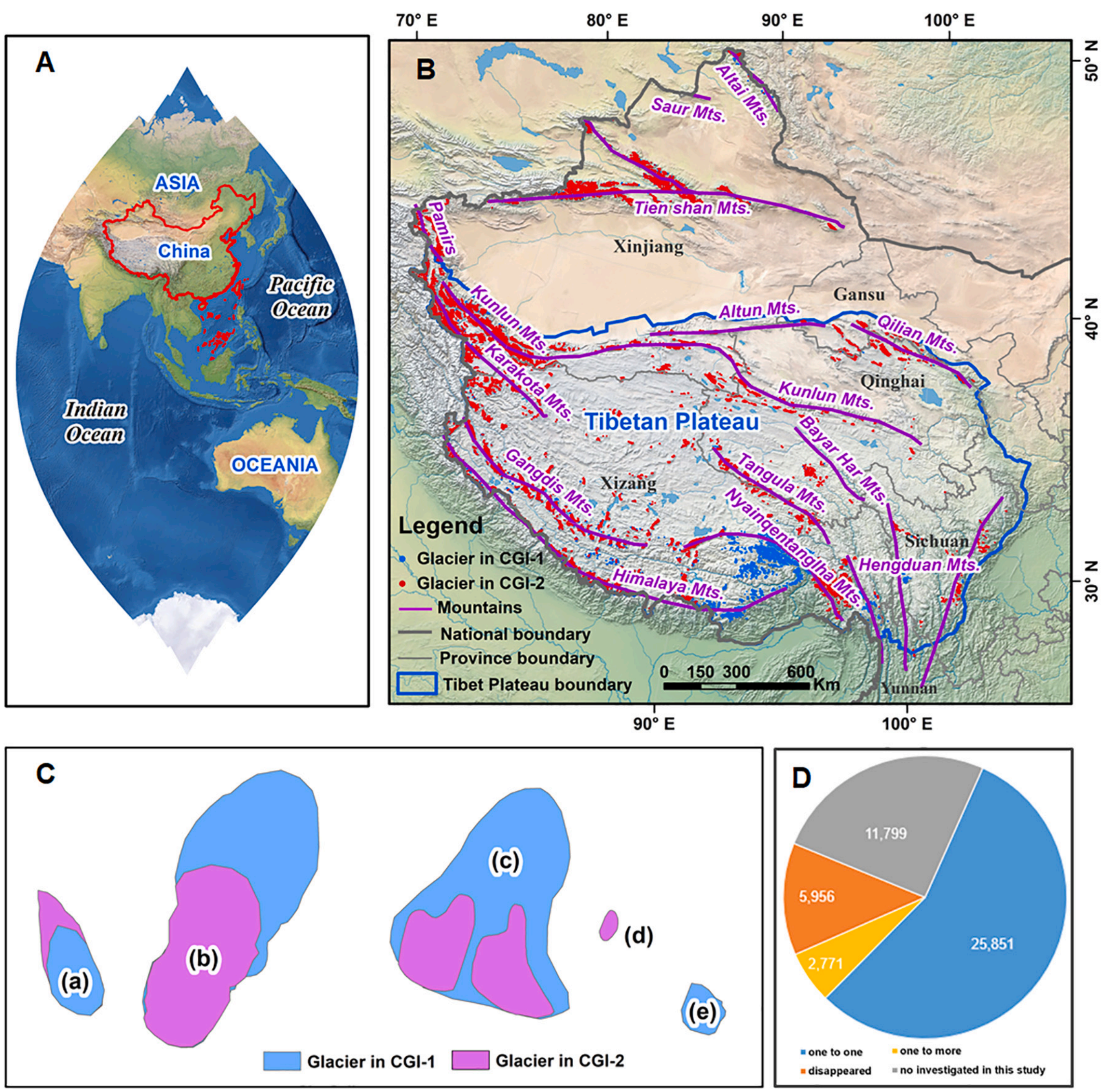


**Fig. 1.** China's glaciers and their evolution during the first (CGI-1, the 1950s-1980s) and second (CGI-2, the 2000s-2010s) Chinese Glacier Inventories. A. Geographical location of China in the world. B. Distribution of glaciers in CGI-1 and CGI-2 as well as their associated mountain ranges and provinces. C. Sketch map of the four types of changes in glaciers from CGI-1 to CGI-2: (a) advanced glacier from one to one; (b) retreated glacier from one to one; (c) glacier division from one to two; (d) not appeared in CGI-1; and (e) disappeared glacier in CGI-2. D. Pie chart for the number of glaciers and different types of glacier evolution.

glacier changes and their influencing factors using a range of approaches, including in-situ measurements, remote sensing, and modelling (e.g., Li et al., 2008; Xiao et al., 2007; Yao et al., 2012a, 2012b; Yao et al., 2019; Yang et al., 2019). These studies have indicated that an overall retreating trend in glaciers has been observed in China during the past half-century (e.g., Ding et al., 2006; Li et al., 2008; Tian et al., 2016; Xiao et al., 2007; Yao et al., 2004; Zhang et al., 2011). The glacial recession in China has profound impacts on the socioecological systems of China, as well as other regions of Asia and even the world, through material and energy flows (IPCC, 2019; Su et al., 2019; Wester et al., 2019). However, in contrast to the overall glacier mass loss and area/volume shrinkage, changes in glaciers in the western Kunlun Mountains, Karakoram, and Pamirs have been very anomalous in recent decades (Hewitt, 2005; Wang et al., 2018; Farinotti et al., 2020). Their glacier mass has lost very little or has even grown (Kääb et al., 2015; Li et al., 2019b), glacier area and volume has presented no significant changes (Bhambri et al., 2013; Ke et al., 2015), and a considerable number of glaciers have advanced or surged (Copland et al., 2011), which is described as the "Karakoram Anomaly" and has received increasing attention (Hewitt, 2005; Bolch et al., 2012; IPCC, 2019; Farinotti et al., 2020).

Continuous in-situ monitoring of glacier change can provide detailed and accurate information on glaciological parameters for a deeper understanding of glacier-climate interactions and glacio-hydrology, and these data are also fundamental for the validation of glacier-related modelling (Zemp et al., 2019; Yang et al., 2019). However, due to the inaccessibility of most glaciated areas and shortages of long-term human and financial resources, only a few glaciers have been observed, and very few glaciers have been continuously monitored as reference glaciers in the world (WGMS, 2020). With the development of remote sensing and geographic information system technologies, monitoring and assessing glacial distribution and associated changes over large scales, such as glaciated mountain ranges and basins and at national scales, have gradually become possible (Paul et al., 2015; Tian et al., 2014; Zhou et al., 2020). To establish a national-scale glacier inventory that also serves as a baseline to identify future changes, the first Chinese Glacier Inventory (CGI-1) were carried out from 1978 to 2002 following recommendations from the International Commission on Snow and Ice for the World Glacier Inventory (WGI) (Shi et al., 2009). In 2006, the Ministry of Science and Technology of China launched the project "Investigation of Glacier Resources and their Changes in Western China". From 2006 to 2012, the second Chinese Glacier Inventory (CGI-2) was implemented (Guo et al., 2015; Liu et al., 2015). CGI-1 and CGI-2 compiled glacier outlines and basic parameters (such as geographic location, area, length, orientation, and elevation) during two different periods (the 1950s-the 1980s and the 2000s-the 2010s), thereby providing critical information for an improved understanding of the distribution and changes in China's glaciers.

Based on CGI-1 and CGI-2, recent studies have analysed glacier changes in the Altai Mountains (Yao et al., 2012b), Qilian Mountains (Sun et al., 2015), Tien Shan Mountains (Xin et al., 2017), and the Silk Road Economic Belt, which lies within China (Li et al., 2019a). However, these studies did not give attention to individual glacial evolution between the two periods. Some glaciers emerged in CGI-2, but statistics were not available for CGI-1 because of the uncertainty of visual interpretation, which may have led to a lower estimate of retreat. Che et al. (2018) quantified glacier changes in the Chinese Tien Shan Mountains by determining the correspondence between glaciers during the periods of CGI-1 and CGI-2, but they did not consider the disappearance and division of glaciers (one to two or more). In addition, Chinese glaciologists, including Yao et al. (2004), Ding et al. (2006), Xiao et al. (2007), Li et al. (2008), Zhang et al. (2011), and Tian et al. (2016), assessed the changes in glaciers at a national scale and provided a largely coherent picture of China's glacier recession in recent decades. However, these studies were mainly based on literature assessments and limited-sample statistical analyses, and a more spatially explicit and coherent assessment of China's glacier changes remains to be conducted.

A wealth of studies has also qualitatively or quantitatively explored the driving factors of China's glacier changes during the last half-century. These studies have generally indicated that glacier shrinkage was mainly caused by a significant increase in air temperature (Li et al., 2011; Wang et al., 2020a; Yao et al., 2012a). Increased precipitation amounts have been observed over most glaciated areas in China; however, these increases in precipitation are far from offsetting the effect of air temperature (Che et al., 2017; Liu et al., 2006). In addition, studies have also revealed that glacial morphology, such as glacier size and debris coverage, as well as topographic conditions within glaciated areas, including elevation, slope, and aspect, has also had a significant impact on the magnitude of changes in glaciers (Zhu et al., 2018a). Nevertheless, a comprehensive analysis of multiple influencing factors remains to be performed.

To address these gaps, we first conducted a spatially explicit and coherent national-scale assessment of glacier changes by establishing a one-to-one correspondence between glaciers from CGI-1 to CGI-2. In that process, we made an effort to discriminate the different types of glacial evolution during CGI-1 and CGI-2, including glacier disappearance, advancement, and division. The identified changes were also quantified at both the individual glacier and glaciated basin scales. Second, we further provided an overview of in-situ observed glacier mass balance and length changes in China. Finally, the influencing factors of glacier evolution encompassing climatology and climate change, as well as glacial morphology and topographic condition, were comprehensively analysed along with a review of previous relevant studies. The knowledge synthesized in this study may benefit various research communities, such as glaciology, cryosphere science, hydrology, ecology, and climate change, and provide a scientific basis for decision-making for regional sustainable development.

## 2. Materials and methods

### 2.1. Glacier inventory datasets and processing

CGI-1 was established based on aerial photographs and topographic maps from the 1960s to 1980s combined with extensively field investigations, and 34 parameters (e.g., area and elevation, etc.) was recorded following the standard guidebook of the World Glacier Inventory (Müller et al., 1977; Shi et al., 2009). The parameter measurement was based on the traditional mapping method, e.g., glacier area was measured by manual planimeter (Guo et al., 2015). Finally, a total of 46,377 glaciers with an area of approximately 59,425.2 km$^2$ in China from the 1960s to 1980s were measured, compiled and published with 21 books and about 200 attached maps in Chinese (Shi et al., 2009). The Chinese Glacier Information System (CGIS) was further developed in 2004 by digitizing the glacier distribution and topographic maps, logging the parameter data from CGI-1, and conducting quality control (Li et al., 2008; Wu and Li, 2011). We only used digitized glacier boundary from CGIS to establish a one-to-one correspondence between glaciers from CGI-1 to CGI-2. All parameters (such as area and elevation) were taken directly from CGI-1 to avoid any digitization error (Wu and Li, 2011). CGI-1 is considered the best and indispensable data for understanding the distribution and basic parameters of China's glacier for the earlier period of time. These datasets were obtained from the Key Laboratory of Remote Sensing of Gansu Province, Chinese Academy of Sciences. Wu and Li (2011) evaluated the accuracy of CGI-1 and found that the area error was less than 5% for most glaciers and less than 10% for almost all glaciers. They concluded that the quality of CGI-1 can meet the requirement of glacier change assessment and the error is largely derived from the limitation of the traditional mapping method.

CGI-2 updated glacier outlines and basic parameters of 85.5% of China's glaciers based on Landsat TM/ETM+, ASTER, and Google Earth images from 2004 to 2011 (Guo et al., 2015; Liu et al., 2015; Kargel et al., 2014). The other 6201 glaciers (24.5%), with an area of 8753.5

km$^2$, are mainly located in the eastern Nyainqentanglha Mountains and western Hengduan Mountains, which are frequently cloudy and covered by snow year-round; thus, no high-quality visible images are available (Guo et al., 2015; Liu et al., 2015) (Fig. 1-B). CGI-2 dataset was publicly available from the National Tibetan Plateau Data Centre of China (https://data.tpdc.ac.cn/en/). Glacier positioning accuracies were validated by comparing the boundaries of some sample glaciers measured by real-time kinematic differential GPS or digitized from high-resolution images. The results showed that the mean glacier positioning errors in CGI-2 were ± 10 m for clean ice and ± 30 m for debris-covered glaciers (Guo et al., 2015). Taking the length of glacier outlines and their positioning accuracies into account, the evaluated area error was ±3.2% for all glaciers but ±17.6% for the 1723 debris-covered glaciers in CGI-2 (Guo et al., 2015). The detailed glacier area errors for each glaciated basin are presented in Table S1.

In this study, we first removed 6201 glaciers from the CGI-1 and CGI-2 datasets because their real-time information was not updated but compiled, after which 40,176 and 42,370 glaciers remained, respectively. Then, we established the correspondence between glaciers from CGI-1 to CGI-2 following different kinds of evolutionary trajectories of modern mountain glaciers. As shown in Fig. 1-C, the evolutionary trajectories of glaciers from CGI-1 to CGI-2 can be divided into four major categories: (1) advanced glaciers from one to one; (2) shrinking glaciers from one to one; (3) glacier division from one to two or more; and (4) disappeared glaciers. We made an effort to discriminate the different types of glacier evolution based on glacier boundaries in CGI-1 and CGI-2 one by one. However, there were 5598 glaciers whose position or outline did not match well, i.e., there were unacceptable errors in CGI-1 and/or CGI-2, or some glaciers emerged in CGI-2, but statistics were not available in CGI-1. After eliminating these 5598 glaciers, we found that 5956 glaciers in CGI-1 disappeared before the implementation of CGI-2, and 28,622 glaciers had evolved into 32,070 glaciers in CGI-2.

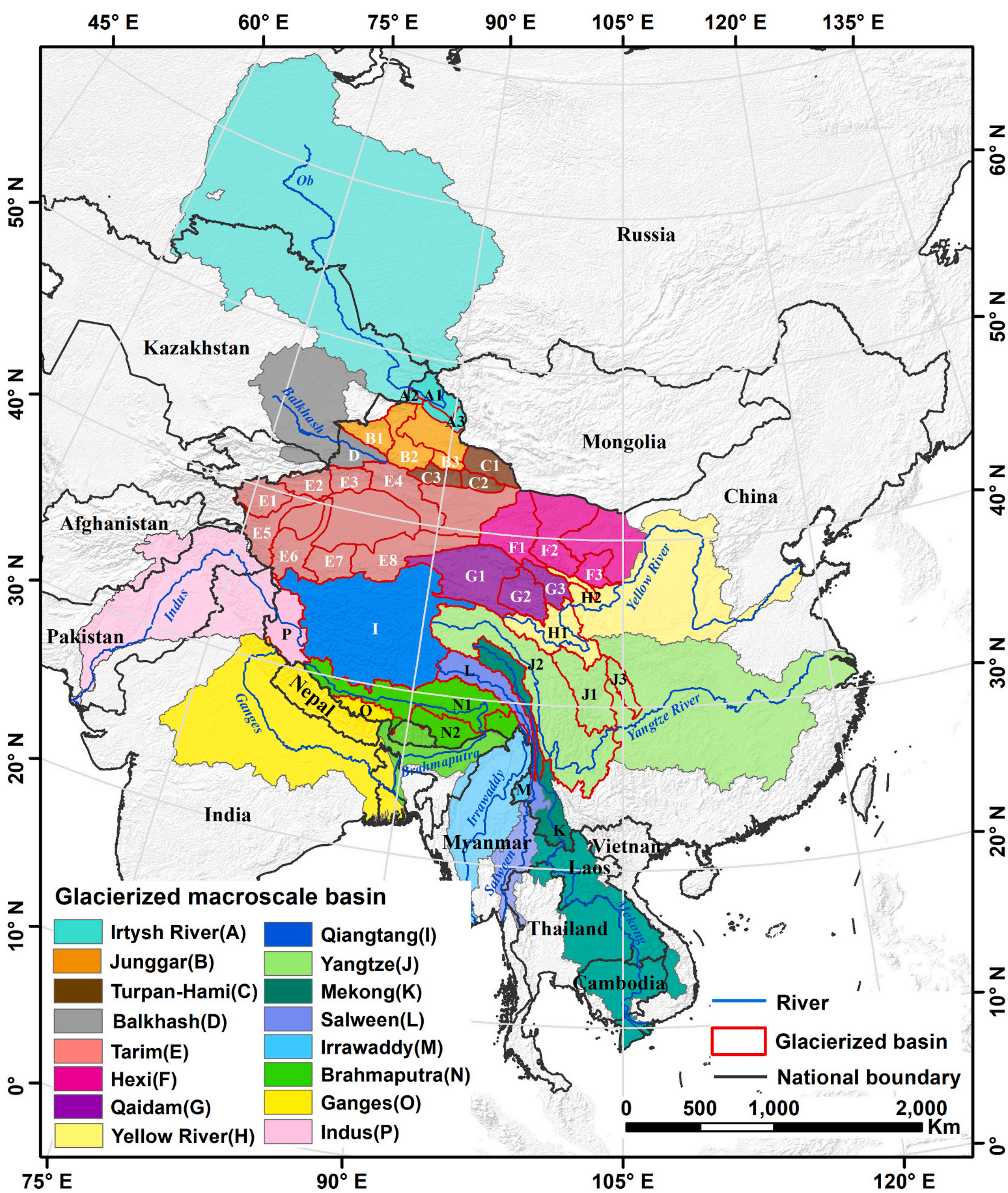


**Fig. 2.** Distribution of China's glaciers and the associated basins and the countries within a basin which is denoted by a letter (and a number sometimes). The white letters indicate endorheic basins while the black letters show exoreic basins. The basin name corresponding to each basin can be found in the Table S1.

### 2.2. Delineation of glaciated basins

We explored glacier changes and their influencing factors on a river basin basis. We first made an intersection between the CGI and river basins, and 37 glaciated basins were identified (Fig. 2). River basin classifications for both China and worldwide were collected from the Data Centre for Resources and Environmental Sciences, Chinese Academy of Sciences (http://www.resdc.cn), and HydroBASINS (www.hydrosheds.org), respectively. The latter is mainly used to determine international river basins which connect with China's glaciated basin boundaries. The glaciated area for each basin, i.e., glaciated unit, was considered based on glacier-covered grids with a spatial resolution of $0.25^\circ \times 0.25^\circ$. The 37 glaciated basins can also be grouped into 16 glaciated macroscale basins. Among them, 7 macroscale GBs (Junggar, Turpan-Hami, Tarim, Hexi, Qaidam, Qiangtang and Ili) are endorheic and the others are exoreic. Six international macroscale GBs are fed by China's glaciers but are shared across borders, i.e., the Ob (Irtysh River), Balkhash (Ili), Mekong, Salween, Irrawaddy, Brahmaputra, Ganges, and Indus.

For all 37 GBs in China, there were notable differences in glacier number and size (Table S1). During the CGI-2 period, the number of glaciers in 15 GBs was more than 1000, and most of them were distributed on the TP. The combined glacier number of the 15 GBs was 41,564, and the total area was 44,688.5 $km^2$, accounting for 85.6% of the number and 86.2% of the area of total glaciers in CGI-2. Both the number and area of glaciers were largest in the Yarlung Zangbo River Basin, i.e., 8135 glaciers with a total area of 10,055.6 $km^2$. The number of glaciers in 9 GBs was less than 100, and their combined number and area were only 507 and 270.8 $km^2$, respectively. Conspicuously, only 1, 5, and 11 glaciers were distributed in the Ulungur River Basin, Fujiang River (a tributary of the Yangtze River) Basin, and Jimunai River Basin, respectively.

### 2.3. Quantification of glacier changes

Glacier changes are characterized not only as changes in surface mass balance (i.e., the difference between accumulation and ablation) and equilibrium line altitude (ELA), the elevation at which accumulation equals melting, but also in area, volume, length, thickness, terminus, flow velocity, and ice temperature (IPCC, 2013; IPCC, 2019). These changes in a glacier can be observed by geodetic and glaciological methods (Zemp et al., 2009; Zemp et al., 2019), or monitored and inverted by remote sensing technologies of satellites, unmanned aerial vehicles, and automatic cameras (Che et al., 2020a; Guo et al., 2015; Huss et al., 2013). Some parameters, including glacier volume and ELA, have also been estimated empirically based on existing parameters (Braithwaite and Raper, 2009; Huss and Farinotti, 2012; Osipov, 2004). Based on the parameters available in CGI-1 and CGI-2, the glacier area and volume parameters and balanced-budget ELA are estimated to quantify their changes at both the individual glacier and river basin scales, respectively. The empirical formula used to calculate glacier volume and ELA, as well as the indicators measuring absolute and relative changes in glaciers, are described in detail here. In-situ observation-based glaciological and geodetic methods for measuring glacier changes are introduced in Section 2.4.

#### 2.3.1. Glacier area and volume

Glacier area is a key parameter in glacier inventories. The glacier area changes are quantified by measuring the annual area change (AAC) and annual percentage of area change (APAC). To quantify the AAC and APAC for each basin, we applied area-weighted time spans (for details see formulas shown in Text S1).

Glacier volume estimation is based on volume-area scaling, which has been widely used to assess regional- and global-scale glacial water resources.

$$V = cA^{\gamma} \tag{1}$$

where $V$ and $A$ are the volume and area of a single glacier, respectively, and c and γ are scaling parameters. Scaling coefficients $c$ and $\gamma$ have been theoretically determined in several previous studies (e.g., Chen and Ohmura, 1990; Bahr, 1997(a); Bahr, 1997(b); and Radić and Hock, 2010) for different periods. In this study, $\gamma = 1.375$ and $c = 0.0365$ are applied to estimate the volume at the single glacier scale. The scaling coefficients were derived from the volume estimates of the world's mountain glaciers and ice caps across 19 glaciated regions (Radić and Hock, 2010) and have been widely adopted for regional- and global-scale studies (e.g., Che et al. (2018)). The uncertainties of scaling coefficients c and γ were evaluated by comparing the results derived by Bahr et al. (1997a) and Bahr (1997b), and the results showed that the mean glacier volume error was ±3.7% in High Mountain Asia (Radić and Hock, 2010), including China.

Similar to the quantification of glacier area changes (Text S1), estimated glacier volume changes are quantified using annual volume change (AVC) and annual percentage of volume change (APVC); simultaneously, area-weighted periods are also applied to quantify the AVC and APVC for each basin.

#### 2.3.2. Median elevation of the glacier (MEG) and equilibrium line altitude (ELA)

Modern ELA for an individual glacier is generally estimated by employing the glaciological mass balance method (Kumar et al., 2020). However, massive human and financial resources are needed to implement mass balance measurements. Glaciologists found that the balanced-budget ELA can be quickly estimated for a glacier inventory using the MEG parameter (i.e., the elevation dividing the glacier area into equal halves) or even by the average value of the maximum and minimum glacier altitudes (i.e., midrange altitude, also called Gefer's method) for cases where the median elevation is not available (Braithwaite and Raper, 2009; Nesje, 1992; Osipov, 2004). In addition, many indirect methods have been used to estimate ELA, such as the Terminus to Headwall Altitude (THAR), Accumulation Area Ratio (AAR), Maximum Elevation of Lateral Moraine (MELM), and Area Altitude Balance Ratio (AABR) (Mehta et al., 2014; Shukla et al., 2018; Kumar et al., 2020).

Both the MEG and THAR methods were applied as a rapid estimate of the balanced-budget ELA for individual glaciers in this study. The THAR method can be described via eq. (2):

$$ELA = E_{min} + \Delta E \times R \tag{2}$$

where $E_{min}$ is the minimum elevation of a glacier and $\Delta E$ and $R$ are the vertical range (i.e., $\Delta E = E_{max} - E_{min}$) and the ratio between the maximum and minimum glacier elevations, respectively. The ratio was between 0.35 and 0.5, and the variations mainly depend on the degree of continentality of conditions (Bakke and Nesje, 2011; Che et al., 2018; Nesje, 1992; Osipov, 2004). A ratio ($R$) of 0.42 is used here following Osipov (2004) and Che et al. (2018).

Similar to the quantification of AAC (Text S1), annual MEG/ELA changes (AMC/AEC) are used to estimate glacier MEG/ELA changes. In addition, an area-weighted period was applied to quantify the AMC/AEC on a river basin scale.

### 2.4. In-situ observations for measuring glacier changes

The glacier mass balance and length are two essential parameters in worldwide glacier monitoring strategies, and an associated monitoring network (i.e., World Glacier Monitoring Service, WGMS) has been built systematically (Zemp et al., 2019). In this study, changes in glacial mass and length were analysed using glaciological and geodetic data mainly from the WGMS, and these data are complemented by newly published assessments. The in-situ observational methods for measuring glacier mass and length changes are described below in detail.

#### 2.4.1. Glacier mass balance

Long-term glacier mass balance is one of the most important parameters for understanding regional climate fluctuations and glacier runoff evolution (Hoelzle et al., 2003; Li et al., 2011). Changes in glacier mass can be observed by both geodetic and glaciological methods (Zemp et al., 2019; Wang et al., 2020a; Mehta et al., 2021; Che et al., 2020b). The geodetic mass balance is determined based on a comparison of glacier surface elevations in different periods (usually over multiyear to decadal periods) from in-situ observations (such as from terrestrial laser scanners) and airborne and spaceborne surveys, and by assuming an ice density of 850 kg/m$^3$. The determination of glaciological mass balance is based on point measurements by using the stake/snow pit methods and then extrapolated to unmeasured areas of the glacier. More details of the methodology can be found in previous studies, such as Zemp et al. (2013).

Generally, the individual point mass balance $b_a$ for a hydrological year (generally from the beginning of October to the end of the next September) can be expressed as follows:

$$b_a = b_w + b_s \tag{3}$$

where $b_w$ represents the accumulation in winter and is measured by the snow-pit method in the accumulation zone and $b_s$ indicates the ablation in summer and is determined by the measuring-stake method in the ablation zone. For one given glacier, the overall mass balance $B$ is calculated as follows:

$$B = \frac{\sum_{i=1}^{n} b_i s_i}{S} \tag{4}$$

where $S$ is the total glacier area, $n$ is the number of isolines of mass balance, and $b_i$ and $s_i$ are the mean mass balance and the total area between adjacent isolines for a glacier, respectively.

There are three main error sources for the glaciological mass balance method, i.e., stake/snow pit-based point measurement, spatial extrapolation, and glacier reference area (Zemp et al., 2015). The uncertainty of point measurement is mainly derived from the failure of equipment operation, snow density measurements, and estimated firn density (Andreassen et al., 2016; Che et al., 2017). Zemp et al. (2013) found that the mean error of field point measurement can reach ±140 mm w.e. per year. The uncertainty of spatial extrapolation depends largely on the interpolation method used, local topography, and the number and distribution of stakes and snow pits (Zemp et al., 2015). The accurate measurement of glacier area is also crucial to the minimization of overall mass balance calculation error (Che et al., 2017).

In this study, changes in mass balance were analysed by collecting all up-to-date glacier mass balance data at the national scale. Because the number of glaciers with long-term mass balance measurements is very limited, a reconstructed dataset of glacier mass balance in China was also applied. Detailed information on the mass balance for the investigated glaciers is shown in Table S2.

#### 2.4.2. Glacier length

Length variations are generally geodetically observed and calculated on a yearly scale by repeated measurements between benchmark locations or glacier termini (Yao et al., 2012a). The measurements of glacier length (also termed terminus or front position) boundaries are easier and more direct to obtain than other glacier parameters during in-situ observations (Che et al., 2017). Similarly, to analyze the changes in glacier length, a national glacier length dataset was established by collecting existing glacier length data (detailed information is shown in Table S3).

The accuracy of glacier length measurements varies greatly by equipment and method, such as geomorphological evidence, topographic maps, stereophotogrammetric surveys, aerial photographs, theodolites, and RTK-GPS (Che et al., 2017). The uncertainty of in-situ front observations through differential global positioning systems can be negligible (Yao et al., 2012a, 2012b). In this study, most glacier length data were obtained from Yao et al. (2012a, 2012b), and their uncertainty was estimated at 5–10%.

### 2.5. Factors affecting glacier change

Generally, regional climatic conditions determine the intensity of glacier ablation and accumulation (i.e., mass balance) over a long time scale to a large extent, and climate change is recognized to be the dominant driver of the world's glacier mass balance and the associated area, volume, and length changes (IPCC, 2019). To explore the climatological influencing factors of glacier area changes, positive degree-day (PDD) and negative degree-day (NDD), snowfall, and rainfall as typical climatic indexes were analysed in this study. Glacial morphology and topographic conditions also play a role in glacier formation and its changes. By summarizing the previous literature and using glacier size and debris coverage as glacial morphological indexes, the latitude, slope, and aspect of glaciated areas as geographic indexes were investigated.

PDD and NDD are measures of the combined duration and magnitude of temperatures above and below freezing, respectively. Snowfall and rainfall were calculated by employing a state-of-the-art parameterization scheme in terms of wet-bulb temperature, relative humidity, pressure, and elevation information (Ding et al., 2014) (a more detailed description is given in Text S2). Daily weather data (including air temperature, precipitation, relative humidity, and surface pressure) and elevation data were employed to investigate PDD, NDD, snowfall, and rainfall. Air temperature, precipitation, and relative humidity were gathered from the daily observational CN05.1 gridded dataset at a spatial resolution of 0.25°, which was interpolated based on 2416 stations in China (Wu and Gao, 2013) and has been widely used in the assessment and validation of climate change at national or subnational scales (Guo et al., 2018; Wang et al., 2020c). Daily surface pressure was obtained from NCEP/NCAR Reanalysis 1 with a spatial resolution of 2.5° × 2.5° (available at https://psl.noaa.gov/data/gridded/data.ncep.reanalysis.html). Elevation data (SRTMDEM) with a spatial resolution of 90 m were provided by the Geospatial Data Cloud site, Computer Network Information Centre, Chinese Academy of Sciences (http://www.gscloud.cn). Due to different spatial resolutions, we further interpolated the surface pressure and elevation datasets to a common resolution of 0.25° × 0.25°. To detect the trend of PDD, NDD, snowfall, and rainfall, Sen's slope was used to estimate the slope of trends (Sen, 1968), and the nonparametric Mann-Kendall trend test was applied to quantify the significance of trends with a confidence level of 95% ($P$ < 0.05) (Mann, 1945; Kendall, 1948). In addition, Pearson's correlation was used to determine the relationship between glacier changes and the associated influencing factors.

## 3. Glacier changes revealed by comparing CGI-1 with CGI-2

### 3.1. General characteristics of glacier evolution

Approximately 74.6% of the glaciers ($n$ = 34,578) in CGI-1 are analysed in detail here, and their total area and volume are 43,665.2 km$^2$ and 3865.2 km$^3$, accounting for 73.5% of the area and 69% of the volume of total glaciers in CGI-1, respectively. The different types of glacier evolution during the periods of CGI-1 and CGI-2, including glacier disappearance, advancement, and division, are determined and explored in this study for the first time (Fig. 1-(C—D), Fig. 3, Table S4).

In summary, 5956 glaciers (17.2%) with a total area of 1127.2 km$^2$ and a total volume of 28.8 km$^3$ disappeared before the CGI-2 period, while the other 28,622 glaciers evolved into 32,070 glaciers in CGI-2 because 2721 glaciers were divided into two or more branches as the glaciers retreated. In addition, approximately 5.5% ($n$ = 1907) of the total number of glaciers advanced, and the total area (volume) increased

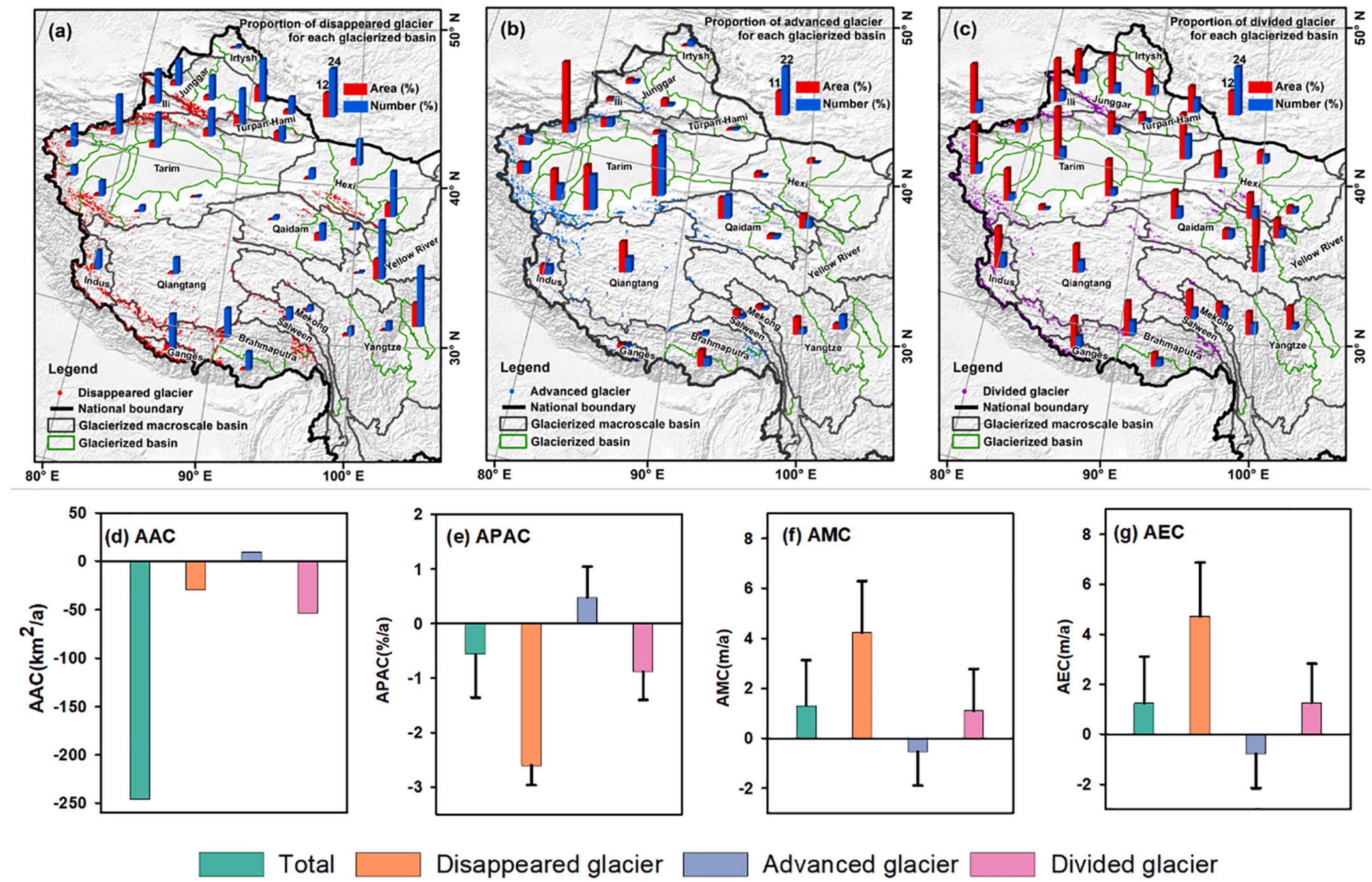


**Fig. 3.** Change in three different types of glaciers in China. (a-c) Spatial distribution of disappeared, advanced and divided glaciers and their proportion in each glacierized basin. (d-k) Absolute and/or relative changes in terms of area, MEG and ELA for the three types of glaciers and all investigated glaciers (green) in this study. Note: The vertical error bars in (e-g) denote the standard deviations of all individual glacier changes. The extinction time of disappeared glaciers is assumed to be the area-weighted average period of CGI-2 at the river basin or national scales. The ELA and MEG are considered the maximum glacier altitudes when a glacier disappears. (For interpretation of the references to colour in this figure legend, the reader is referred to the web version of this article.)

from 4541.3 km$^2$ (498.0 km$^3$) to 4915.4 km$^2$ (540.2 km$^3$) during the area-weighted average period from CGI-1 (1969.9) to CGI-2 (2008.6), i. e., increased by 374.1 km$^2$ (42.2 km$^3$), with an AAC(AVC) of 96.6 km$^2$/decade (11.1 km$^3$/decade) and an APAC(APVC) of 4.8%/decade (7.4%/decade). The combined area (volume) of all 34,578 investigated glaciers across China decreased from 43,650.0 km$^2$ (3865.2 km$^3$) to 34,152.9 km$^2$ (3078.3 km$^3$) during the area-weighted average period between CGI-1 and CGI2, i.e., decreased by 9497.1 km$^2$ (−786.9 km$^3$) with an AAC (AVC) of −2461.2 km$^2$/decade (−203.8 km$^2$/decade) and an APAC (APVC) of −5.6%/decade (−5.3%/decade). Taking glaciers with no investigation in CGI-2 ($n = 10{,}300$) and nonupdated glaciers in CGI-2 ($n = 6201$) into consideration, it was estimated that all glaciers in China decreased with an AAC of −3599.1 km$^2$/decade and AVC of −298.3 km$^3$/decade over the past decades.

The MEG and ELA increased as glaciers shrank based on reductions in area and volume (Fig. 3 and Fig. 4). Our results show that the average MEG (ELA) of all investigated glaciers increased during the area-weighted average period between CGI-1 and CGI-2, with an AMC of 13.1 m/decade and AEC of 12.5 m/decade; thus, the MEG and ELA increased by approximately 65.5 m and 62.5 m from 1961 to 2010, respectively. Based on the higher retreating rate and faster reductions in area and volume, the MEG and ELA of disappearing glaciers increased much faster than those of the other types, even with the assumption that their extinction time was equal to the area-weighted average period of CGI-2. The amplitude of retreat in terms of area and volume for divided glaciers was larger than the overall change rate of all investigated glaciers across China during the same period. For the advanced glaciers, their average MEG (ELA) decreased slightly between CGI-1 and CGI-2, with an AMC of −5.4 m/decade and AEC of −7.9 m/decade.

### 3.2. Spatial pattern of glacier changes

Fig. 4 presents the spatial pattern of China's glacier changes in terms of area, volume, MEG, and ELA for all 34,578 investigated glaciers from the CGI-1 to CGI-2 periods at both the individual glacier and basin scales. The spatial distributions of different types of glaciers and their proportions in terms of the number and area for all investigated glaciers at the glaciated basin scale are also shown in Fig. 3(a-c). These data provide spatially explicit information at national-scale glacier changes during the past half-century. In general, the retreating rate is the smallest in the interior of the TP, which has consistently lower magnitudes of AAC, AVC, APAC, APVC, AEC, and AMC (Ding et al., 2006; Li et al., 2008; Tian et al., 2016; Xiao et al., 2007) (Fig. 4). The proportion of advanced glaciers is large across the interior of the TP (Fig. 3(b)), and a large proportion of disappeared and divided glaciers are mainly distributed in the areas surrounding the interior of the TP (Fig. 3(a, c)).

The interior of the TP includes the Karakoram Mountains, Pamirs and the Kunlun Mountains, and the Tanggula Mountains, in which the APAC and APVC of a considerable number of glaciers are more than −5%/decade or even positive and the AMC and AEC are less than 10 m/decade or even negative. The region consists of GBs that include the Qiangtang, Hotan, Keriya, Qarqan, Yarkant, and western Qardam basins, all of which exhibited lower rates of glacier shrinkage with an average APAC ranging from −3.8%/decade (Yarkant) to −0.4%/decade

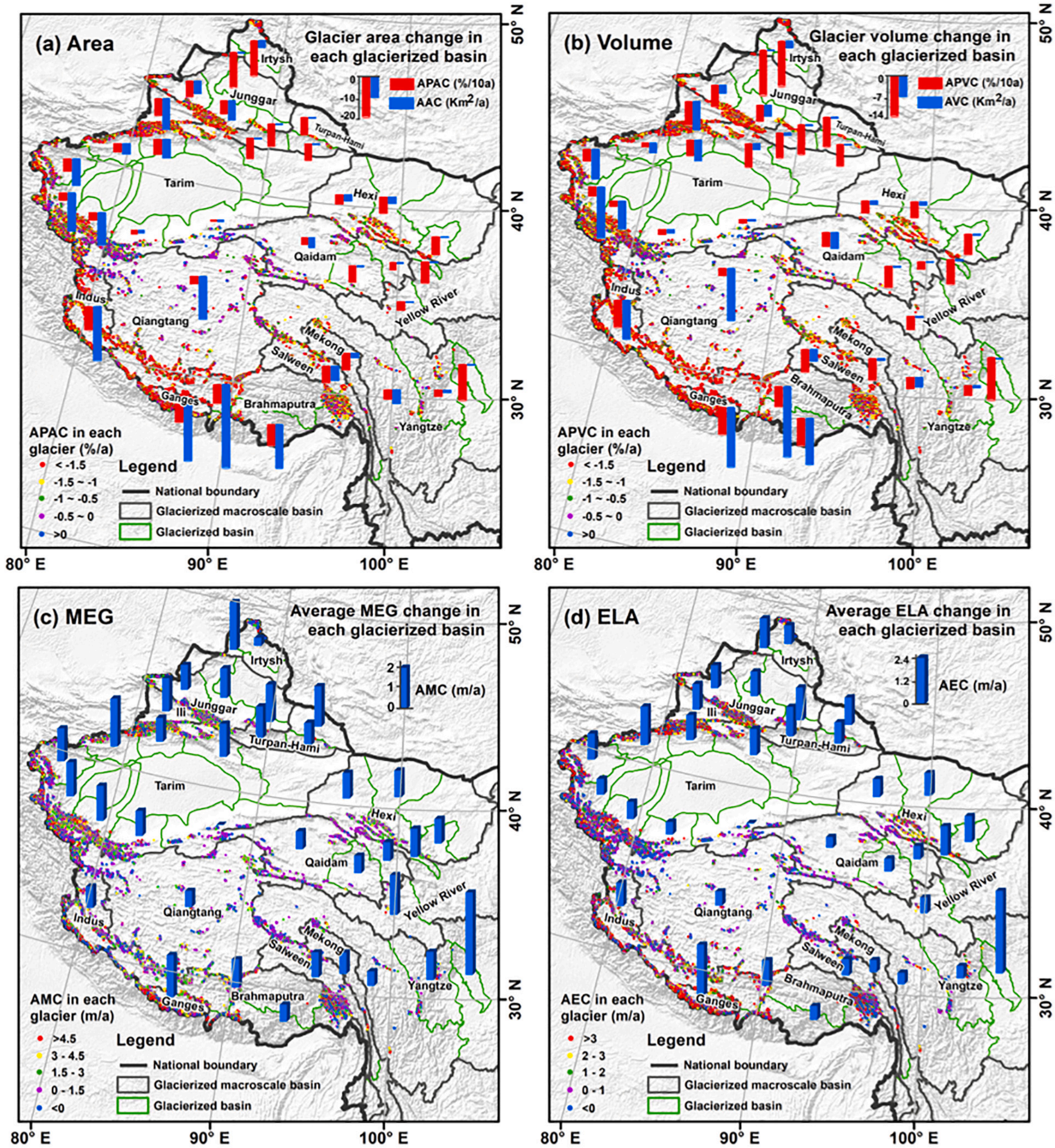


**Fig. 4.** Relative and/or absolute changes in terms of the (a) area, (b) volume, (c) MEG and (d) ELA for all investigated glaciers at both individual glacier and basin scales across China during the CGI-1 and CGI-2 periods.

(Qarqan) and average APVC varying between −5.4%/decade (western Qardam) and − 1.6%/decade (Qarqan). For the 6 GBs, the average AEC varies between 0.4 m/decade (Qarqan) and 9.8 m/decade (Hotan), and the AMC have overall the same pattern as the AEC. For most GBs in the interior of the TP, the proportions of disappeared and divided glaciers are less than 5% and 10%, respectively, although the proportion of advanced glaciers can reach 36.5% (Qarqan).

Extending to the mountain ranges surrounding the interior of the TP, the rates of glacier shrinkage across most GBs are more than the average rate in China, with an average APAC/APVC less than −5%/decade and average AEC/AMC more than 10 m/decade. In particular, 16 GBs exhibited a drastic area reduction with an average APAC of less than −7%/decade (Table S5), most of which originated from the northern and eastern Tien Shan Mountains, eastern Qianlian Mountains, Altai Mountains, and Himalaya Mountains. For these regions, the proportion of disappeared glaciers is very large, with more than 10–20% of glaciers disappearing during the past half-century and few glaciers advancing over the northwestern GBs of China. However, the glaciers developed in the southwestern Tien Shan Mountains, eastern Kunlun Mountains, western Hengduan Mountains, and West Qilian Mountains, including the GBs containing Qinghai Lake, Min River, Shule, Aksu, Jinsha River, and Yellow Riverhead, exhibited a lower area and volume reduction, and their average APAC was more than the average APAC in China (−5.6%/decade). In these regions, the proportion of advanced glaciers is large, and the proportion of disappeared glaciers is small. The spatial patterns of APVC, AMC, and AEC are generally consistent with those of APAC. In addition, a large proportion of divided glaciers are mainly distributed in GBs in North Xinjiang, as well as the western and southern margins of the TP.

The absolute retreat extent is reflected in the indicators AAC and AVC, and it is not significantly correlated with the relative retreat extent due to the heterogeneity of glacier number, area, and volume. Compared with the spatial patterns of APAC and APVC, the amplitudes of AAC and AVC are large in the Himalaya Mountains, Gangdis Mountains, Karakoram Mountains, western Kunlun Mountains, and western Tien Shan Mountains, in which the AAC of most GBs is less than $-100$ km$^2$/decade and AVC is less than $-10$ km$^3$/decade (Table S5). Instead, the extent of AAC is small in the GBs, especially originating from the northern and eastern Tien Shan Mountains, eastern Qianlian Mountains, and the Altai Mountains, in which the AAC is not less than $-10$ km$^2$/decade and AVC is more than $-1$ km$^3$/decade (Table S5). Furthermore, the proportion of disappeared and divided glaciers is small in the interior of the TP; however, their absolute number and area are considerably large.

## 4. In-situ observation-based glacier changes

### 4.1. Changes in glacier mass balance

The first measurement of mass balance in China was carried out at Urumqi Glacier No. 1 in 1958 (Li et al., 2011; Xiao et al., 2012). Mass balance was observed in-situ for 43 glaciers; however, continuous observations over at least 10 years were only performed for 8 glaciers, i.e., Urumqi Glacier No. 1, Qiyi, Meikuang, Xiao Dongkemadi, Hailuogou, Baishui No. 1, Zhadang, and Kangwure (Table S2). Among them, Urumqi Glacier No. 1 has been continuously monitored for more than 40 years and is the only glacier that is included in the WGMS network as the

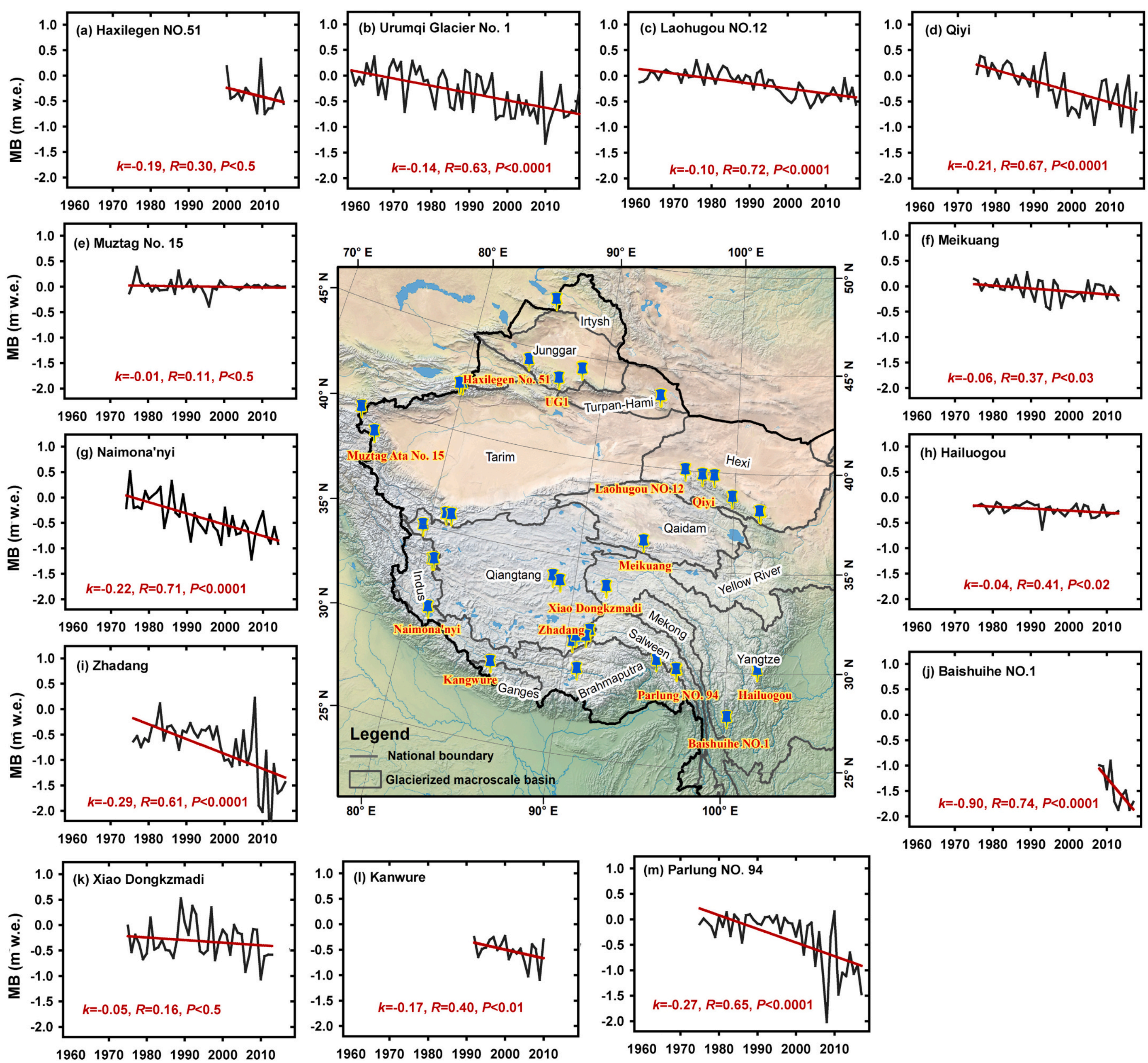


**Fig. 5.** In-situ observed and reconstructed glacier mass balance (MB) in China. Glaciers with MB data is unevenly distributed in each river basin as shown in the central figure. The labels show the 13 glaciers that have mass balance series with no less than 10 years, and their MB series are presented and regressed linearly in surrounding plots, where "*k*", "*R*" and "*P*" denote the slope of regressed line (unit: m w.e./10a), regression coefficient and their significance level, respectively. Data sources for each glacier are shown in Table S2.

world's reference glacier (Li et al., 2011; Xiao et al., 2012; Xu et al., 2019). In addition, a long-term mass balance time series has been reconstructed in China in recent years for some glaciers, such as the Parlung NO. 94, Zhadang, Muztagh No. 15, Haxilegen No. 51 and Lao-hugou glaciers, based on short-term mass balance measurements as presented in the Methods section. In summary, a total of 13 glaciers have mass balance series with no less than 10 years in China (we consider them the reference glaciers of China hereafter).

Fig. 5(a-l) shows the annual changes in net mass balance for 43 glaciers at each macroscale glaciated river basin based on in-situ observations along with reconstructed data for some periods. The results show that the mass balance of most observed glaciers was characterized by apparent fluctuations before the 1990s, which were characterized by a lower average annual mass loss or even gain in many observation years, but the mass loss has intensified vigorously since the 1990s and is characterized by a substantially increased thinning rate and relatively small fluctuation in most river basins (Che et al., 2017; Wang et al., 2020a). One exception is in the southwestern Tarin and northwestern Qiangtang River basins, i.e., the interior of the TP, especially in the eastern Pamir, the glaciers of which showed stability or small mass fluctuation, i.e., no significant trend. Glacial mass loss was the lowest here, and the mass balance was even positive. Taking Muztag glacier No. 15 as an example, the average annual mass balance values were 0.023 and 0.029 m w.e./decade during the 1975–2016 and 2000–2016 periods, respectively (Zhu et al., 2018b). The other exception is in the source regions of the Yellow River and Yangtze River, as well as the southern Qaidam Basin, which are mainly distributed in the Bayan Har Mountains and Tanggula Mountains. The glaciers in these places presented a lower mass loss, and the negative trend from 1975 to the present was not statistically significant at the 0.05 significance level. Significantly, glacial mass deficits have occurred in other regions. The most negative mass balance occurred on the southwestern TP over in recent decades, such as Parlung NO. 94 and Baishuihe NO.1, whose average annual mass balance values were approximately −1.463 and −0.994 m w.e. from 2008 to 2017. Based on the remote sensing method, Wu et al. (2018) found that the glaciers in the Kangri Karpo Mountains experienced a mean mass loss of −0.710 m w.e./decade from 2000 to 2014 (Wu et al., 2018). The rate of accelerated melting was also largest on the southwestern TP from 1975 to 2017. The magnitude and rate of glacial mass loss gradually decreased from the southwest to the interior (northwest) on the TP (Yang et al., 2019; Yao et al., 2012a).

Northern Xinjiang (including the Chinese Tien Shan Mountains) shows a moderate mass loss. The annual mass loss for most investigated glaciers was less than 0.6 m w.e. during the period from the 1990s to 2010s, although the mass loss decreased from northeast to southwest. Urumqi Glacier No. 1 in the northern Chinese Tien Shan Mountains has the longest mass balance record in China, and the mass balance decreased by −0.142 m w.e./decade ($P < 0.0001$) during the period from 1959 to 2019. In addition, both the monitoring on site and remote sensing results show that the mass loss has slightly decreased over the latest decade (the 2010s) after the accelerated retreat since the 1990s in most of this region; however, it is necessary to further confirm whether the decrease will continue (Wang et al., 2020a).

To put the estimated mass changes in the Chinese glaciers into a global perspective, the mean annual mass balance of reference glaciers is used (WGMS, 2020). As shown in Fig. 6, for all 13 reference glaciers in China, the negative trend of mass balance was −0.135 m w.e./decade during the 1960–2019 period, which was slightly larger than that of 41

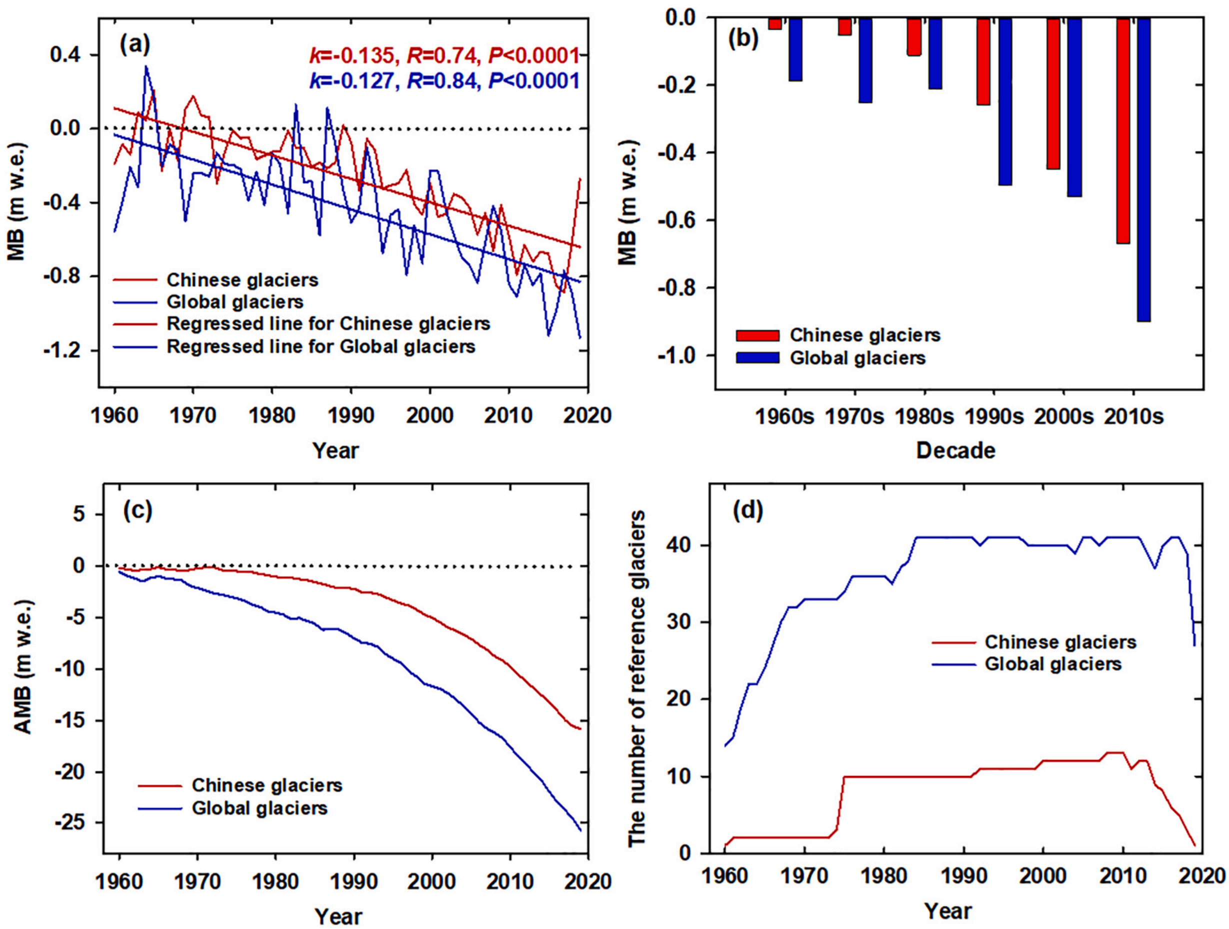


**Fig. 6.** Comparison of the annual (a) and decadal (b) average mass balance (MB), (c) accumulative mass balance (AMB) and (d) the associated number of reference glaciers with long-term time series observations between China and the globe.

reference glaciers globally (−0.127 m w.e./decade) in the same period. However, the mean mass loss rate of Chinese reference glaciers in any decade was lower than that observed worldwide. From 1960 to 2019, the accumulative mass balance of the reference glaciers in China and worldwide reached −15.8 and − 25.8 m w.e., respectively. For the mid-low latitudes of the world, the mean rate of glacier mass loss was the lowest in High Mountain Asia, including China (Zemp et al., 2019; IPCC, 2019; Li et al., 2019c).

### 4.2. Changes in glacier length

As shown in Fig. 7, considerable spatiotemporal changes in glacier fronts were observed in China in recent decades. Glacier retreat has occurred since at least 1917 in China; for example, the front of the Ata glacier in southwestern China (Brahmaputra River Basin) continuously retreated −2300 m by 2006, and the shrinkage in this region was also the most drastic. For example, the retreating rates of the Yanong 70 and Xibu glaciers reached 730 and 480 m/decade during the 1980–2001 and 1970–1999 periods, respectively. Wu et al. (2018) investigated 1166 glaciers in the Kangri Karpo Mountains recognized from satellite images and found that only 9 glaciers experienced a mean advance of 148 m/decade from 1985 to 2015, while 86 glaciers experienced a mean retreat of 759 m (217 m/decade) ranging from 60 to 39,560 m/decade; furthermore, the retreat has accelerated since 2000 (Wu et al., 2018). Following the changes in the glacier area, volume, and mass balance, the shrinkage reflected in glacier length also decreased from the southwest to the interior (northwest) on the TP and increased from the northeast to the southwest in northern Xinjiang, including the Chinese Tien Shan Mountains, during the past half-century (Yao et al., 2012a). The retreating rate was the lowest in the eastern Pamir and Karakoram Mountains, and advances have been found for a considerable number of glaciers there, i.e., "Karakoram Anomaly" (Farinotti et al., 2020; Hewitt,

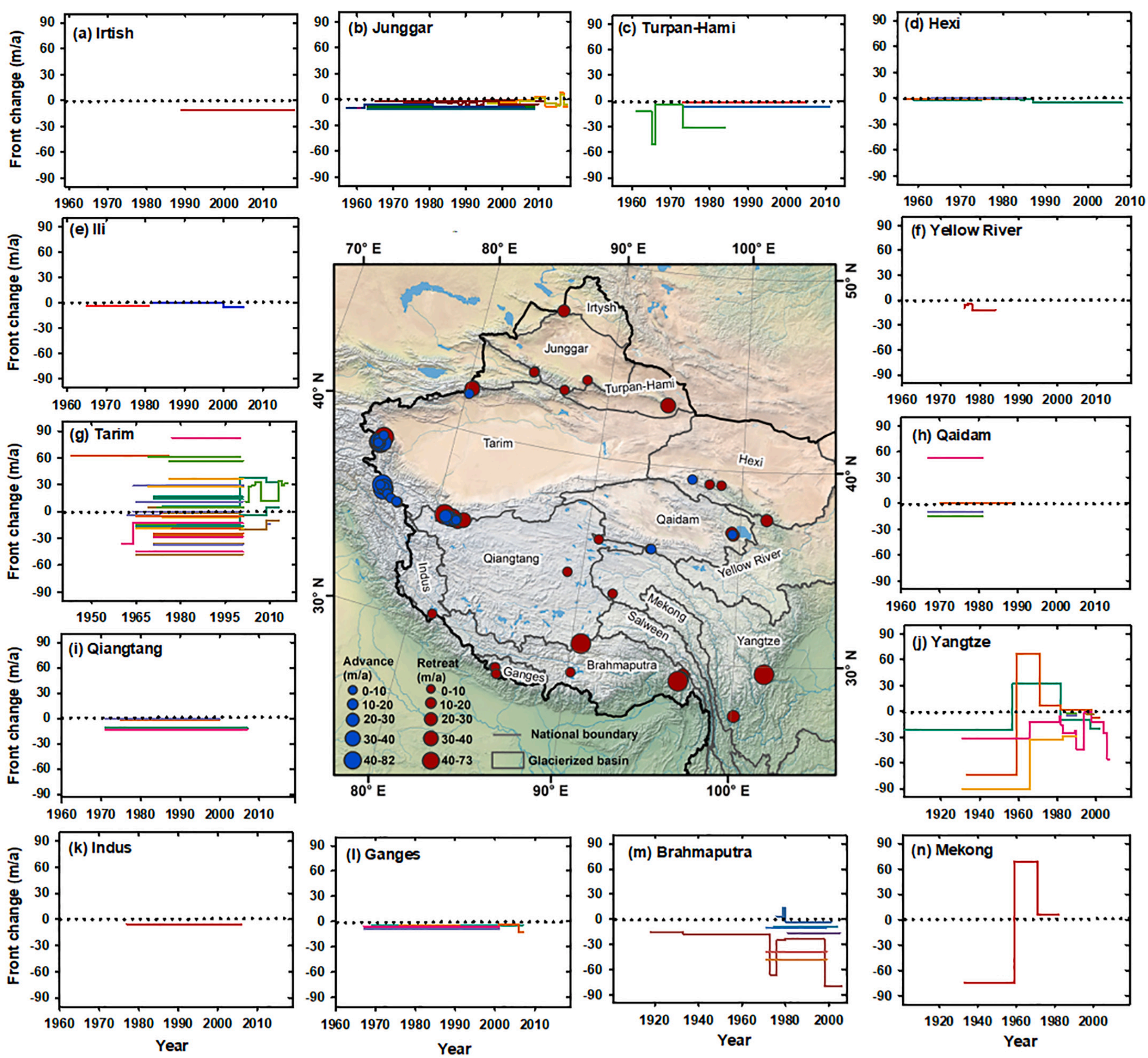


**Fig. 7.** In-situ observation-based changes in glacier length (front) during the past half-century on a river basin scale. The straight lines in each river basin refer to the average change rate in individual glacier length in the corresponding periods. Data sources for each glacier are shown in Table S3.

2005).

## 5. Influencing factors for glacier changes

### 5.1. Climatic conditions and changes

The climatic conditions of glaciated areas are not only dominated by large-scale atmospheric circulation systems but are also profoundly determined by the topography of glaciated areas, such as elevation, aspect, and latitude (more detailed information is provided in Section 5.2). The air temperature and precipitation amount are particularly important climatic indicators for assessing glacier change, although other variables such as solar radiation, wind, and humidity can also play a role. Glacial ablation generally occurs when the air temperature is positive; therefore, PDD and NDD are the two most effective indexes to measure the thermal conditions for glacier melting and storage (Hock, 2005). Lower and decreasing negative NDD is beneficial for glacier storage in a colder environment, while higher and increasing positive PDD can accelerate glacier melting (Che et al., 2018). The precipitation amount can be essential for the input of glacier mass; however, snowfall and rainfall have distinct effects on glacier mass balance. The presence of snowfall is beneficial to the formation and development of glaciers by increasing the surface albedo and through mass accumulation. In contrast, rainfall accelerates glacier retreat through changes in the surface energy budget, such as the reduction in the surface albedo and the release of latent heat (Flanner et al., 2011; Ding et al., 2014; Ding et al., 2017; Tamang et al., 2019).

#### 5.1.1. Climatic conditions

Fig. 8 shows that the observed climatology of PDD, NDD, snowfall, and rainfall is heterogeneous across China's GBs; furthermore, there are large differences in climatic conditions between the glaciated unit and downstream areas for each glaciated basin. In the period from 1961 to 2010, the annual mean PDD ranged from 148.6 °C to 3719.9 °C across

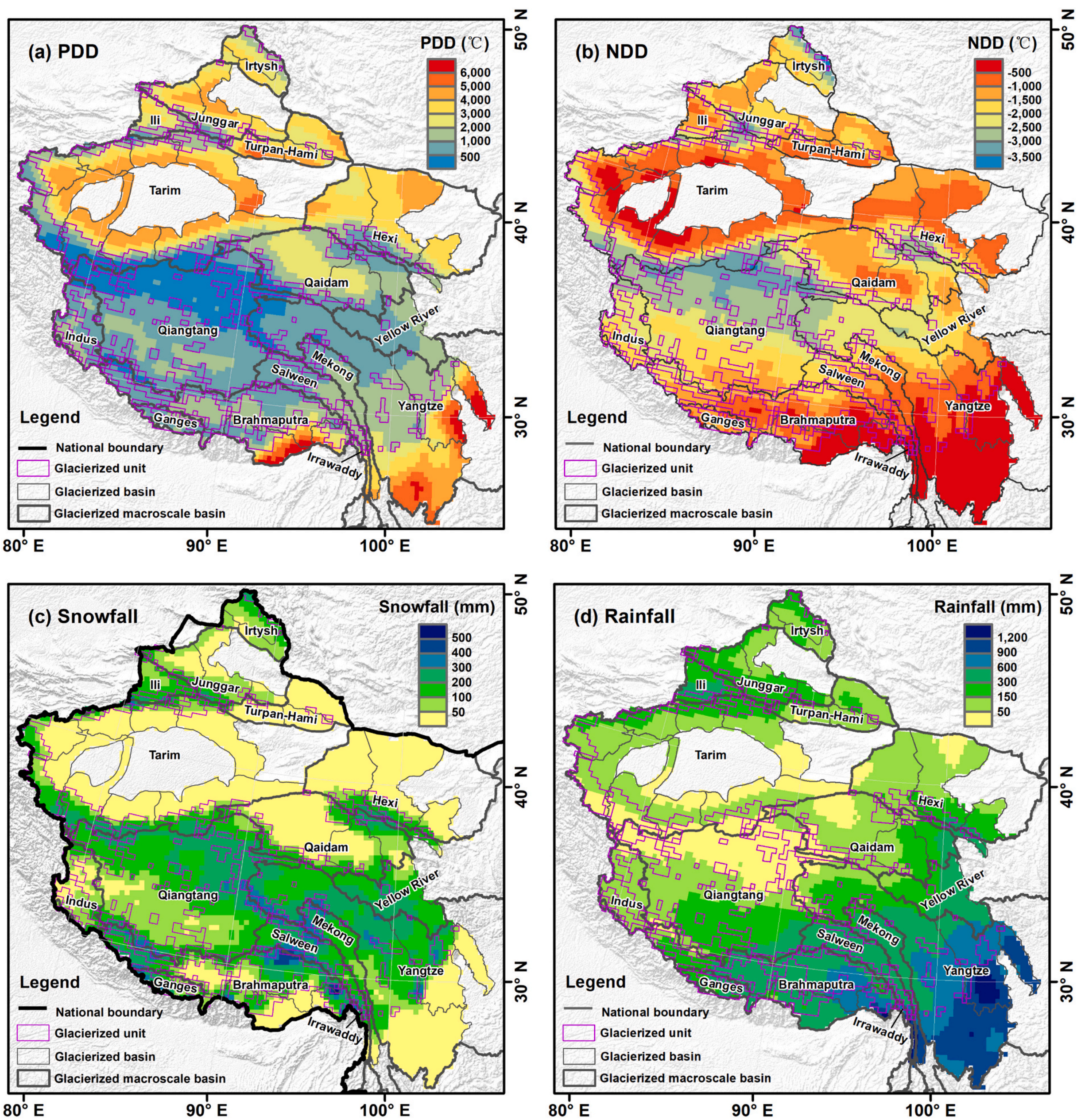


**Fig. 8.** Climatology of the (a) positive degree-day (PDD), (b) negative degree-day (NDD), (c) snowfall and (d) rainfall across glacierized basins (GBs) during 1961–2010.

the glaciated units of China. At the glaciated basin scale, during the average CGI-1 and CGI-2 periods, the mean PDD was highest in the eastern Tien Shan Mountains, including glaciated units of the Bayi, Hami, East-range, and Turpan River basins, followed by the Jimunai and Aibi Lake River basins, both of which are located in the northern Chinese Tien Shan Mountains. The mean PDD was also higher on the southeastern TP, especially in the glaciated unit of the Fujiang, Zangnan, Min, and Irrawaddy River basins. However, the mean PDD was relatively low across most glaciated units on the TP, especially in the interior of the TP (Fig. 8(a)). The mean NDD absolute value was highest in the glaciated unit in the Irtysh River Basin (northernmost GUs of China, less than −3370 °C), followed by the glaciated unit in the interior of the TP (including the glaciated areas of the Qardam, Qarqan, Hotan, Keriya, etc.). However, the mean absolute value was lowest in the glaciated units on the southeastern TP, followed by the eastern Tien Shan Mountains (Fig. 8(b)). For snowfall, the annual mean value varied from 10.2 mm to 517.0 mm, with a high mean value on the southeastern TP and in the Irtysh River Basin (more than 200 mm) and the lowest mean value in the eastern Tien Shan Mountains (less than 50 mm) (Fig. 8(c)). For liquid precipitation, the annual mean rainfall ranged from 0 to 1065.8 mm, and the mean value was highest in the glaciated units on the eastern TP and in the Ili River Basin, while the lowest values were mainly distributed in the interior of the TP (less than 100 mm), followed by the glaciated units in northwestern Xinjiang (Fig. 8(d)). At a glaciated basin scale, the climatology of PDD has a significant negative correlation with APAC/APVC and a significant positive correlation with AMC/AEC. The APAC/APVC has a positive correlation with snowfall and a negative correlation with rainfall, although they are not significant. A significant positive correlation is observed between AMC/AEC and the climatology of NDD; and the AAC/AVC/APAC/APVC has a negative correlation with

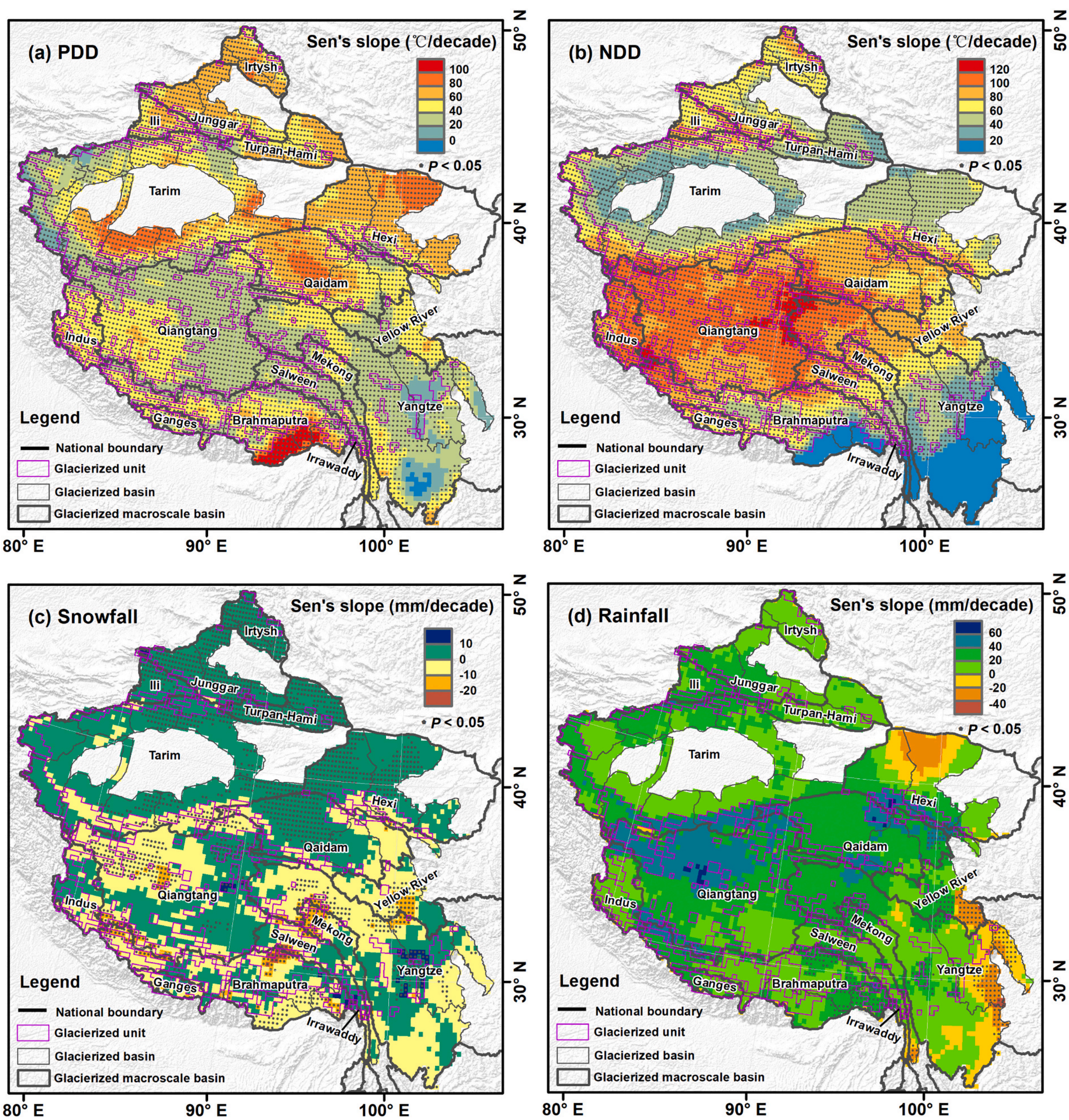


**Fig. 9.** Spatial distribution of Sen's slopes for the (a) positive degree-day (PDD), (b) negative degree-day (NDD), (c) snowfall and (d) rainfall across China's glacierized basins (GBs) from 1961 to 2010. Black points in the grid cell centre indicate that the slope is statistically significant at the 0.05 significance level using the nonparametric Mann-Kendall trend test.

the climatology of NDD, but they are not significant (Table S6).

Generally, if the PDD is large and the rainfall is high, then these glaciated units can be characterized as having a high intensity of ablation. If the NDD is low and snowfall is high, then the intensities of accumulation are high, and vice versa. In China, glaciated units with high ablation and low accumulation are concentrated in the Turpan-Hami, Junggar, and Jimunai River basins. The intensity of both ablation and accumulation is high in the glaciated units on the eastern TP, such as the Yarlung Zangbo, Zangnan, Irrawaddy, Salween, and Mekong River basins. The glaciated units in the Irtysh and Ulungur River basins are characterized by high intensities of accumulation and medium ablation, while the glaciated units with low accumulation and ablation are mainly located in the interior of the TP. In the macroscale Hexi Inland River Basin, the intensity of accumulation gradually increases, and the intensity of ablation decreases from the southeast (Shiyang River basin) to northwest (Hei River and Shule River basins). The combination of the climatology in terms of glacier ablation and accumulation is almost consistent with the magnitude of glacier retreat.

#### 5.1.2. Climate change

As Fig. 9(a-b) shows, the increasing trends of PDD and NDD were very significant over the most glaciated basins and almost all glaciated units from 1961 to 2010, indicating that glacier melting was accelerating and that their protective effect from cold storage (i.e., low-temperature environments) had weakened. During the CGI-1 and CGI-2 periods, the mean slopes of PDD and NDD across all China's glaciated units increased by 46 °C and 78 °C/decade, respectively. At a glaciated basin scale, the increasing slope of PDD was more than 60 °C/decade for 10 GBs, and most of them are located in the eastern Tien Shan Mountains and Qilian Mountains, as well as Qardam. However, the slope was lower in most GBs in the western Tien Shan Mountains and northernmost China. The NDD trend had a significant negative correlation with the climatology of the PDD ($R$ = -0.50, $P < 0.05$), i.e., these GBs with a higher PDD had a smaller increase in NDD, such as across the eastern Qianlian Mountains and eastern Tien Shan Mountains (<60 °C/decade), while the increase in NDD was large in the GBs with a lower PDD (colder storage environment), especially in the GBs in the Karakoram Mountains and Kunlun Mountains (>90 °C/decade). In recent decades, the snowfall on most glaciated units in northwestern China (especially the Irtysh River Basin and northern Tien Shan Mountains) has presented an increasing trend ranging from 1 to 10 mm/decade, although the decreasing trend is significant across most glaciated units on the TP, especially in the Yarlung Zangbo, Mekong, Salween, and Ganges River basins, with mean slopes of −15, −14 and − 14 and − 10 mm/decade, respectively (Fig. 9(c)). A higher increase in snowfall occurred in the GBs with a high PDD ($R$ = 0.52, $P < 0.05$). The liquid precipitation has increased to varying degrees over all China's glaciated units except for the glaciated areas in the Fujiang River Basin (−21 mm/decade) (Fig. 9(d)). The fastest increase in rainfall occurred in the GBs on the southeastern TP (such as the Yarlung Zangbo, Salween, Zangnan, Mekong, and Jinsha River basins) and Ili River Basin. These GBs with a higher increase in snowfall had a smaller increase in rainfall ($R$ = -0.55, $P < 0.05$) (Table S6).

Concerning the changes in intensities of glacier ablation and accumulation, the climatic conditions with higher ablation (or accumulation) were more conducive to ablation (or accumulation) across most glaciated units in Northwest China; however, the increases in mass accumulation were far from offsetting the increased ablation. Climate change over almost all glaciated units on the TP has gradually become increasingly detrimental to glacier accumulation and promotes glacier ablation. One exception is the glaciated area in the Fujiang River Basin, which is characterized by extremely high ablation and low accumulation, although the relevant climatic changes helped minimize glacier retreat during the past half-century. At a glaciated basin scale, a significant positive correlation is observed between AAC/AVC and the trends of snowfall, and a significant negative correlation is observed with the trends of rainfall. No significant correlation between glacier changes and the trends of PDD and NDD was found (Table S6), indicating that there is no simple linear relationship between them at a large regional scale (Li et al., 2019c).

### 5.2. Glacial morphology and topographic conditions

#### 5.2.1. Glacial morphology

As shown in Fig. 10(a), large glaciers are concentrated in most GBs in the western Chinese Tien Shan Mountains and on the TP except GBs in the Zangxi, Mekong, and Salween. The average glacier area is largest in the Muzat River Basin (2.3 km$^2$), followed by the Aksu River Basin (2.1 km$^2$). Most glaciers in the eastern and northern Tien Shan Mountains, Altai Mountains, and East Qianlian Mountains are small. The average glacial area is the smallest in the Ulungur River Basin (0.15 km$^2$), followed by the Fujiang River Basin (0.17 km$^2$). We further categorized the glaciers into six classes: minimal (<0.2 km$^2$), small (0.2–0.5 km$^2$), medium (0.5–1 km$^2$), large (1–5 km$^2$), very large (5–10 km$^2$), and super glacier ($\geq$ 10 km$^2$). Fig. 11 (a-b) presents the proportion of the number (a) and area (b) for all investigated glaciers across different size classes at the basin scale. The percentages of disappeared glaciers in all investigated glaciers in terms of number and area are shown in Fig. 11(c-d). We find that the sizes of almost all 5956 disappeared glaciers are small in all GBs of China, and their average area is only 0.19 km$^2$. In addition, there are significant positive correlations between APAC/APVC and glacier sizes at both individual glacier and glaciated basin scales, such as correlation coefficients between APAC and glacier size of 0.13 ($P < 0.01$) at the individual glacier scale and 0.46 ($P < 0.01$) at the glaciated basin scale. The smaller the glacier is, the easier it is to retreat, i.e., lower APAC/APVC and higher AEC/AMC (Huss and Hock, 2018). However, large AAC and AVC are mainly contributed by large glaciers (Fig. 11 (e-f)). The negative correlation between AAC and glacier size is very significant at both individual glacier ($R$ = 0.40, $P < 0.01$) and glaciated basin ($R$ = -0.37, $P < 0.01$) scales.

In general, if the debris layer over a glacier is thick, solar radiation is significantly blocked from the glacier surface, and glacial melting slows exponentially with increasing thickness, although the rate of melting rises when debris cover is thinner than 2 cm (Benn et al., 2012; Juen et al., 2014; Östrem, 1959). Fig. 10(b) shows that high coverage areas by debris (hereafter debris coverage) are concentrated in the western Chinese Tien Shan Mountains, Karakoram Mountains, Kunlun Mountains, and Himalaya Mountains. At a glaciated basin scale, the debris coverage is largest in the Aksu River Basin, where the debris area accounts for 13.0% of the glacier area during the CGI-2 period, followed by the Kaxgar River (10.4%), Muzat (10.1%), and Min River (9.6%) basins. The debris coverage is 0 for 8 GBs (Fujiang, Jimunai, eastern Qardam, Datong, Bayi, Turpan, Ulungur, and Irrawaddy River basins) and less than 1% for 15 GBs (e.g., Qinghai Lake and Mekong River basins). There is a significant positive correlation between debris coverage and glacier size, and their correlation coefficient can reach 0.72 ($P < 0.01$) at a glaciated basin scale. A negative correlation between glacier retreat and debris coverage is also found; for example, the correlation coefficients between APAC and debris coverage are 0.25 ($P > 0.05$) and 0.11 ($P < 0.01$) at the glaciated basin and individual glacier scales, respectively. An observational study in the Karakoram also showed that debris-covered ice melts slower than debris-free ice and that the melting rate increases with decreasing debris cover (Muhammad et al., 2020).

#### 5.2.2. Topographic conditions

Overall, the mean elevation of China's glaciers increases from north to south, and the glaciers with a peak elevation are located in the Karakoram Mountains, western Kunlun, Himalaya Mountains, and Gangdis Mountains (Fig. 12(a)). At the glaciated basin scale, the average mean elevation of glaciers is highest in the Zangxi River Basin (5895.8 m) during the CGI-2 period, followed by the Qiangtang Plateau (5825.9 m), Ganges (5776.4 m), and Keriya (5707.5 m) River basins. Instead, the

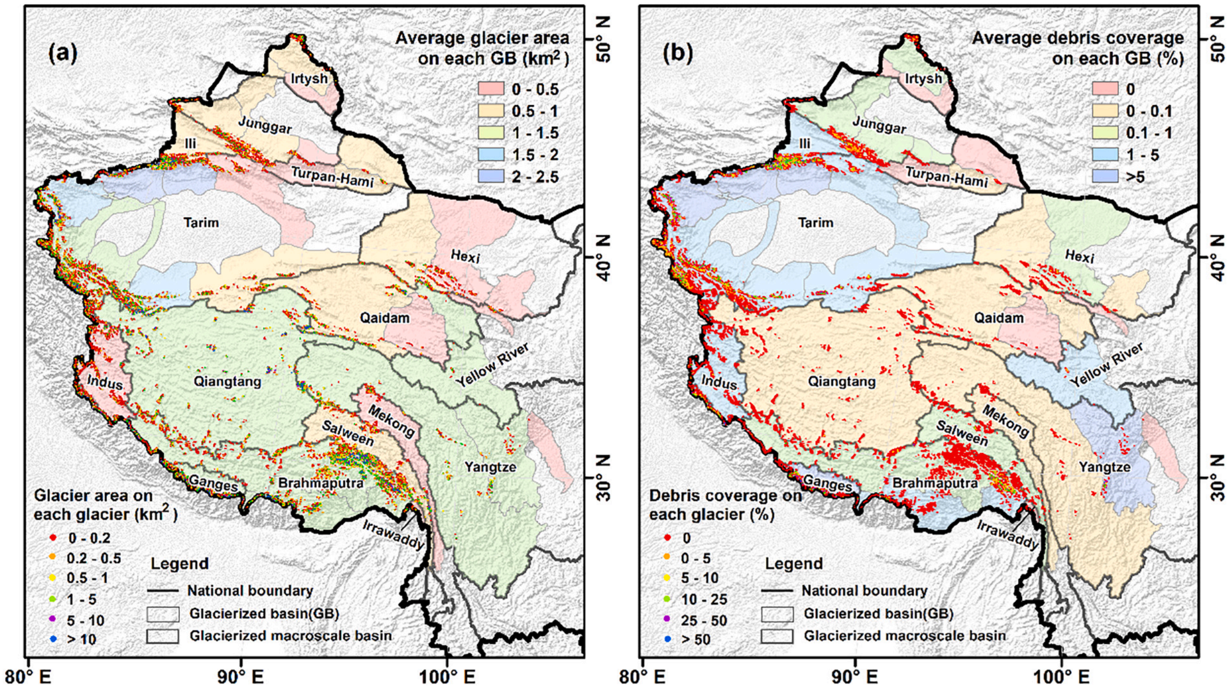


**Fig. 10.** Spatial distribution of glacial morphology in terms of (a) glacier size and (b) debris coverage at both individual glacier and basin scales in China during the CGI-2 period.

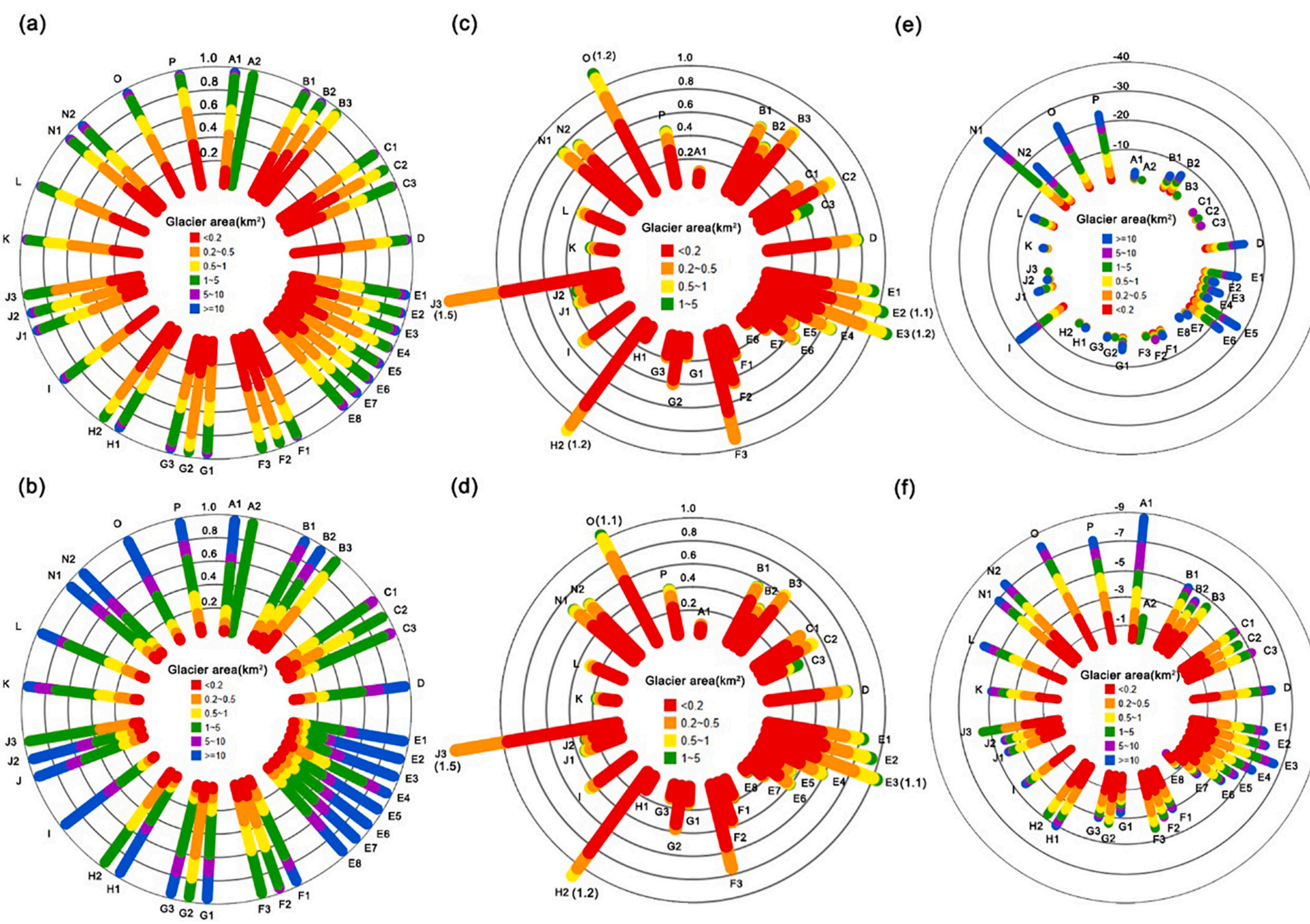


**Fig. 11.** Proportion of the number (a) and area (b) for all investigated glaciers, percentage of the number (c) and area (d) for disappeared glaciers, and AAC (e) and APAC (f) for all investigated glaciers across different size classes at the basin scale.

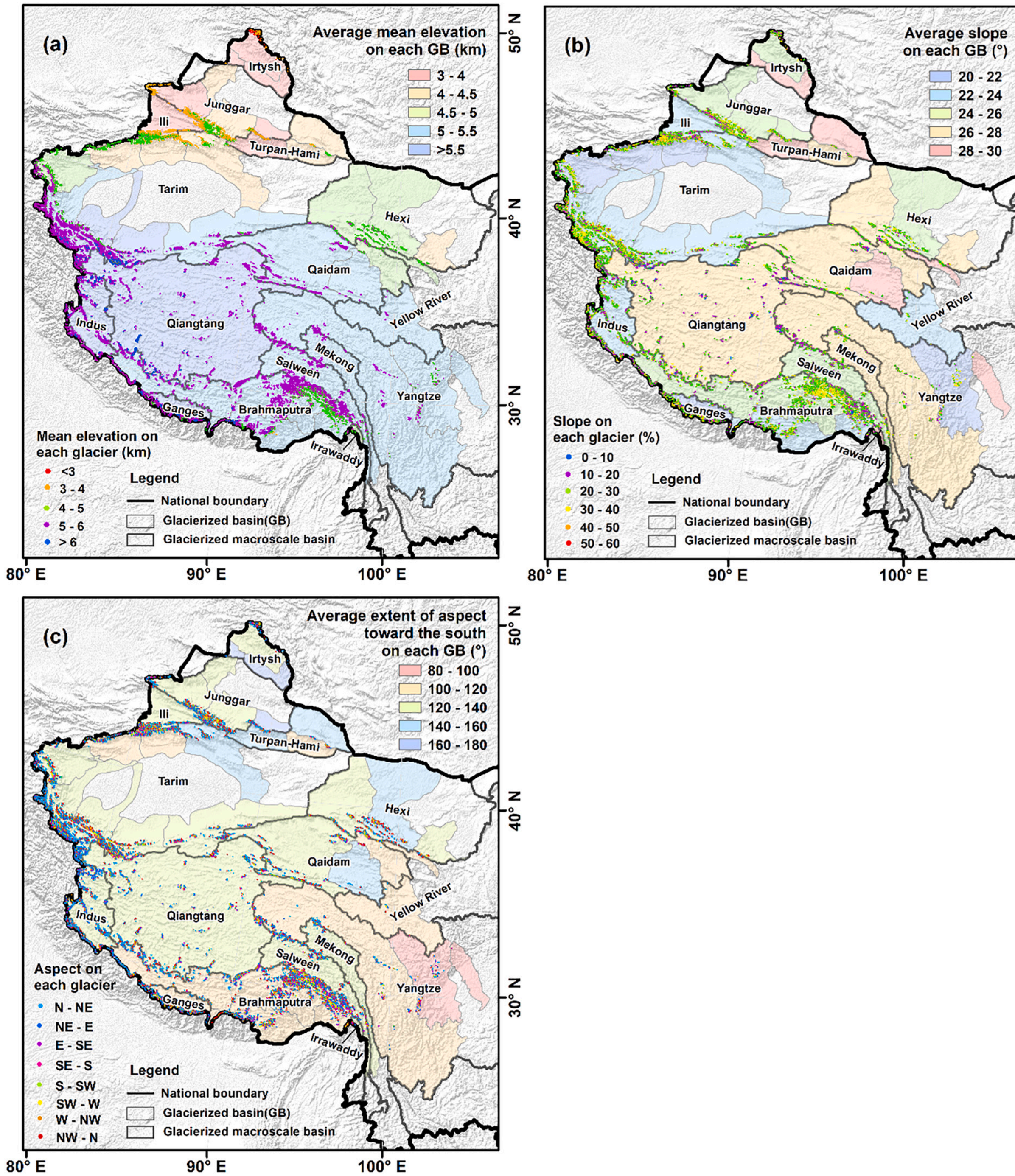


**Fig. 12.** Spatial distribution of topographical conditions in terms of (a) mean elevation, (b) slope and (c) aspect at both individual glacier and basin scales in China during the CGI-2 period. On a basin scale, the average extent of aspect toward the south rather than the aspect itself is shown.

mean elevation in the Altai Mountains is lowest, followed by the northern and eastern Tien Shan Mountains. At high latitudes, the conditions are generally unfavourable for glacial storage but decrease glacier ablation. Elevation within glaciated areas affects glacier changes primarily because of the changes in climatic conditions, especially air temperature. Our results show that the mean elevation has a significant negative correlation with the climatology of PDD ($R$ = -0.68, $P < 0.01$) but a significant positive correlation with the climatology of NDD ($R$ = 0.34, $P < 0.05$) at a glaciated basin scale. In addition, as the elevation rises, the amount of snowfall generally decreases ($R$ = -0.60, $P < 0.01$). Consequently, high-intensity glacier retreat generally first occurs in glaciers at low altitudes, as there is a significant positive correlation between the APAC and mean elevation at both the glaciated basin ($R$ = 0.48, $P < 0.01$) and individual glacier scales ($R$ = 0.04, $P < 0.01$).

The slope within glaciated areas has a significant impact on glacial movement and glacier storage. Generally, if the slope is large, it is not beneficial for glacier storage but promotes glacier movement. Fig. 12(b) shows that there is an irregular distribution for the slope. The average slope within glaciated areas is largest in the Fujiang River Basin (30.2°), followed by the Aksu (29.6°) and Muzat (29.3°) River basins. In contrast, the average slope in the Jimunai River Basin is the smallest (21.1°), followed by the Jinsha River (22.2°) and Qiangtang (22.3°) basins. Our results show that slope has a significant correlation with glacier retreat at an individual glacier scale; for example, the correlation coefficient between the APAC and slope is −0.17 ($P < 0.01$). At the glaciated basin scale, the slope also has a negative correlation with APAC and APVC ($R = 025$ and 0.21, respectively, $P > 0.05$) and a significant positive correlation with AEC/AMC ($R > 0.64$, $P < 0.01$).

Fig. 12(c) shows that the spatial distribution of the aspect within China's glaciers is disconnected. Similar to elevation, the aspect within glaciated areas exerts an influence on the intensity of glacier ablation by mainly affecting climatic conditions, such as solar radiation and air temperature. Theoretically, stronger solar radiation occurs on the southern slope. Our results show that the cold storage effect tends to be weak ($R = -0.52$, $P < 0.01$), and rainfall ($R = -0.53$, $P < 0.01$) and snowfall ($R = -0.34$, $P < 0.05$) increase on the southward slope at the glaciated basin scale. The results also show that aspect correlates with glacier retreat at both the glaciated basin and individual glacier scales, but they are not significant. A recent observational study also found that a south-facing glacier was characterized by the highest mass loss (on average ~ 25% more) in the Karakoram (Muhammad et al., 2020).

### 5.3. Mechanisms of accelerated glacier shrinkage and the "Karakoram Anomaly"

The climatic conditions across western China are mainly influenced by three atmospheric circulation systems. Among them, the western and northern regions (such as Xinjiang) are dominated by westerlies along with the influences of the Siberian anticyclonic circulation, in which climatic conditions are continental because it is situated in the Eurasian hinterland and far from any ocean (Aizen et al., 2001; Panagiotopoulos et al., 2005; Chen et al., 2016). The southern region is deeply affected by the strong Indian monsoon system in summer but the westerlies in winter (Yao et al., 2012a). In addition, the east and southeast are mainly affected by the East Asian monsoon (Yao et al., 2012a; Liu et al., 2015). Yao et al. (2012a) demonstrated that the systematic differences in glacier changes across the TP over the past 30 years were closely related to the increasing/decreasing precipitation in the eastern Pamir/Himalayan regions, which probably resulted from the strengthened westerlies and weakening Indian monsoon, respectively. In the Tien Shan Mountains, the precipitation and associated snow accumulation decreased abruptly in the 1970s, thereby amplifying glacier mass loss along with an increasing temperature, which was mainly attributed to the changes in the North Atlantic and North Pacific in the 1970s through a teleconnection with the westerlies (Cao, 1998).

Observation-based glacier mass loss has generally accelerated, especially since the 1990s, which could be explained by the following mechanisms: 1) increased air temperature during the melting season (Li et al., 2011; Su et al., 2015; Che et al., 2018), 2) increased rainfall and its proportion among precipitation in some glaciated areas, such as the southwestern TP (Ding et al., 2017; Che et al., 2018), 3) reduced albedo on the glacier surface along with the expansion of the ablation zone and deposition of light-absorbing impurities (such as black carbon and mineral dust) (Li et al., 2011; Dumont et al., 2012; Farinotti et al., 2015; Kang et al., 2020; Di Mauro, 2020; Zhang et al., 2021), 4) increased glacial temperature, especially for continental-type glaciers (Li et al., 2011; Ding et al., 2019), and 5) glacier fragmentation, especially for maritime-type glaciers (Du et al., 2013; Su et al., 2015; Wang et al., 2020b).

The "Karakoram Anomaly" is centred on the western Kunlun Mountains but also covers part of the Karakoram and Pamir Mountains and appeared at least as early as the 1970s (Wang et al., 2018; IPCC, 2019). The anomaly has been mainly attributable to decreased summer air temperatures, increased snowfall, and the low-temperature sensitivity of debris-covered glaciers (Archer and Fowler (2004); Farinotti et al., 2020; Bonekamp et al., 2019; De Kok et al., 2020; Shean et al., 2020). However, the anomaly may be unlikely to persist in the future due to the projected increase in air temperature across the region (Kraaijenbrink et al., 2017; IPCC, 2021).

## 6. Summary

To explore the distribution and changes of China's glaciers, two Chinese Glacier Inventories (CGI-1 and CGI-2) have been constructed by Chinese glaciologists in different periods over the past half-century, and an increasing number of glaciers have also been monitored by on-site instruments since the late 1950s. This study performed a reanalysis of the first and second inventories and reviewed the existing in-situ observation-based studies on glacier mass balance and length to provide new insights into national-scale glacier changes and the associated influencing factors across China. We examined the detailed characteristics of China's glacier evolution and spatiotemporal pattern during the last half-century. The influencing factors of glacier changes in terms of climatology and climate change, as well as glacial morphology and topographic conditions, were further mapped and analysed comprehensively. The main results are summarized as follows:

1) We first established a one-to-one correspondence between glaciers from CGI-1 (the 1950s - the 1980s) to CGI-2 (the 2000s - the 2010s) to explore the changes in 34,578 glaciers (74.6% of 46,377 in CGI-1) in China. The results revealed that 5956 small glaciers (17.2% of 34,578) with a total area of 1127.2 $km^2$ have disappeared during the past half-century. The other 28,622 glaciers evolved into 32,070 glaciers in CGI-2 because 2721 glaciers were divided into two or more branches as the glaciers retreated. Among them, approximately 5.5% ($n = 1907$) of the total number of glaciers examined advanced, with an average AAC of 96.6 $km^2$/decade.
2) Weighted by time and area, we estimated that all China's glaciers decreased by an average AAC of −3599.1 $km^2$/decade and AVC of −298.3 $km^3$/decade, with an AEC of 12.5 m/decade from 1970 to 2009, and their APAC and APVC were − 5.6%/decade and − 5.3%/decade, respectively.
3) In-situ observation-based glacier length has decreased since the 1960s on average, and the trend has accelerated since the 1990s. Taking 13 and 41 glaciers with a long-term time series as reference glaciers for China and the globe, respectively, the negative trend of mass balance for Chinese glaciers from 1960 to 2019 was estimated to be slightly larger than that of the global mean, but the mean mass loss for China in any given decade was lower than that of the global mean.
4) The changes in China's glaciers have divergent regional trends dominated by different causes. Overall, the shrinkage during the past half-century increased from the northwest (interior) to southeast on the TP and decreased from the northeast to the southwest in northern Xinjiang, including the Chinese Tien Shan Mountains. The severe glacier shrinkages across the southeastern TP was characterized by the highest mass loss, high APAC/APVC and AEC/AMC, as well as large quantities of disappeared and divided glaciers, which was mainly attributable to higher PDD, NDD, and rainfall, a large decrease in the ratio of snowfall to overall precipitation, and large glacier number and area. The sharp shrinkages across the eastern and northern Tien Shan Mountains, Saur Mountains, and eastern Qianlian Mountains were characterized by the highest APAC/APVC/AMC/AEC and the largest proportion of disappeared and divided glaciers, which was mainly due to the high PDD with relatively low elevation and low snowfall and small glacier number and area. However, glaciers in the interior of the TP and the southwestern Chinese Tien Shan Mountains were relatively stable and characterized by relatively low mass loss and APAC/APVC/AMC/AEC, as well as small quantities of disappeared and divided glaciers but large numbers of advanced glaciers. The possible explanations include climatic conditions with low PDD, NDD, and rainfall, as well as high elevation and large debris coverage.
5) In general, at the glaciated basin scale, climatic conditions (climatology of PDD, NDD, snowfall, and rainfall) are the primary causes of divergent spatiotemporal patterns of glacier change, as reflected in

APAC/APVC/AMC/AEC, mass balance, and length. On the basin scale, a significant positive correlation was observed between AAC/AVC and snowfall changes, and a significant negative correlation was observed with rainfall variations. No significant correlation between glacier changes and PDD and NDD variations was found. Moreover, at both the individual glacier and/or glaciated basin scales, all/some indicators of glacier change had significant correlations with glacier size, debris coverage, mean elevation, slope, and aspect. This indicates that local-scale glacial morphology and topographic conditions exert profound impacts on changes in individual glaciers.

Overall, the estimated spatial pattern of glacier changes in China was consistent with those reported in recent studies derived from geodetic remote sensing observations, including satellite laser altimetry such as the Ice, Cloud, and Land Elevation Satellite (ICESat) (Kääb et al., 2012), satellite gravimetry measurement such as Gravity Recovery and Climate Experiment (GRACE) (Xiang et al., 2021), digital elevation model (DEM) differencing from satellite stereo-imagery (Brun et al., 2017; Bhattacharya et al., 2021), and satellite glacier extent extraction from Landsat images (Li et al., 2008; Tian et al., 2016). These can be considered to be an indirect verification of our results by comparing CGI-1 with CGI-2. Furthermore, our study presents the spatial pattern of China's glacier change with unprecedented detail, over the time span of almost five decades, and at both individual glacier and glaciated basin scales.

In-situ observations of glaciers in China, especially continuous observations, are still limited, which restricts the development of glacier research, especially modelling. The implementation of CGI-1 provided indispensable information on the distribution and basic parameters of China's glaciers during the 1950s-the 1980s, despite the large uncertainties associated with the traditional method. CGI-2 provided updated information on the distribution and changes in China's glaciers. However, the information of approximately 6201 glaciers distributed on the southeastern TP has not been updated, and the accuracy in CGI-2 in general still needs to be improved. To advance research on China's glacier changes further, there is a strong need to continue glacier mapping with a remarkably high quality (Nie et al., 2021). In particular, the newly planned national glacier inventory (CGI-3) should be implemented to explore the most recent glacier changes since 2000. In addition, it is of great importance to strengthen and coordinate in-situ and remote sensing observations and to improve numerical models in the future.

## Author contributions

Cunde Xiao, Deliang Chen, Bo Su and Yanjun Che designed the study; Bo Su, Hongyu Zhao, Yi Huang, Mingbo Zou, Yanjun Che, Rong Guo and Xuejia Wang analysed the data; Bo Su and Yi Huang prepared the figures; Bo Su wrote the manuscript with the major contributions from Deliang Chen and Cunde Xiao. All authors contributed to the interpretation of findings, provided revisions to the manuscript, and approved the final manuscript.

## Declaration of Competing Interest

The authors declare that they have no conflict of interest.

## Acknowledgements

We acknowledge the observed and constructed glacier mass balance data partially provided by Dr. Meilin Zhu and Dr. Huabiao Zhao from the Institute of Tibetan Plateau Research, Chinese Academy of Sciences, Dr. Hui Zhang, Dr. Chunhai Xu, and Dr. Jizu Chen from the Northwest Institute of Eco-Environment and Resources, Chinese Academy of Sciences, Prof. Ninglian Wang and Dr. Anan Chen from the Northwest University of China. We thank Prof. Lizong Wu from the Polar Research Institute of China for helpful discussion on the development and processing of CGI-1. We are also grateful to editors and four anonymous reviewers for their professional comments and suggestions. This research was jointly funded by the National Natural Science Foundation of China (NSFC grant Nos. 41690145 and grant Nos. 42101135) and the Strategic Priority Research Program of the Chinese Academy of Sciences (Grant No. XDA20060401), National Foundation of China Scholarship Council (Grant No. 201906040104), and the Jiangxi Provincial Natural Science Foundation, China (No.20202BAB213013).

## Appendix A. Supplementary data

Supplementary data to this article can be found online at https://doi.org/10.1016/j.earscirev.2022.103926.

## References


Aizen, E.M., Aizen, V.B., Melack, J.M., et al., 2001. Precipitation and atmospheric circulation patterns at mid-latitudes of Asia. Int. J. Climatol. J. R. Meteor. Soc. 21 (5), 535–556.

Andreassen, L.M., Elvehøy, H., Kjøllmoen, B., et al., 2016. Reanalysis of long term series of glaciological and geodetic mass balance for 10 Norwegian glaciers. Cryosphere 10 (2), 535–552.

Archer, D.R., Fowler, H.J., 2004. Spatial and temporal variations in precipitation in the Upper Indus Basin, global teleconnections and hydrological implications. Hydrol. Earth Syst. Sci. 8 (1), 47–61.

Azam, M.F., Kargel, J.S., Shea, J.M., et al., 2021. Glaciohydrology of the Himalaya-Karakoram. Science eabf3668.

Bahr, D.B., 1997. Global distributions of glacier properties: a stochastic scaling paradigm. Water Resour. Res. 33, 1669–1679.

Bahr, D.B., Meier, M.F., Peckham, S.D., 1997. The physical basis of glacier volume-area scaling. J. Geophys. Res. Solid Earth 102, 20355–20362.

Bakke, J., Nesje, A., 2011. Equilibrium-Line Altitude (ELA). In: Singh, V.P., Singh, P., Haritashya, U.K. (Eds.), Encyclopedia of Snow, Ice and Glaciers. Springer Netherlands, Dordrecht, pp. 268–277.

Benn, D.I., Bolch, T., Hands, K., et al., 2012. Response of debris-covered glaciers in the Mount Everest region to recent warming, and implications for outburst flood hazards. Earth Sci. Rev. 114 (1–2), 156–174.

Bhambri, R., Bolch, T., Kawishwar, P., et al., 2013. Heterogeneity in glacier response in the upper Shyok valley, northeast Karakoram. Cryosphere 7 (5), 1385–1398.

Bhattacharya, A., Bolch, T., Mukherjee, K., et al., 2021. High Mountain Asian glacier response to climate revealed by multi-temporal satellite observations since the 1960s. Nat. Commun. 12 (1), 1–13.

Bolch, T., 2017. Asian glaciers are a reliable water source. Nature 545, 161.

Bolch, T., Kulkarni, A., Kääb, A., et al., 2012. The state and fate of Himalayan glaciers. Science 336 (6079), 310–314.

Bonekamp, P.N., de Kok, R.J., Collier, E., et al., 2019. Contrasting meteorological drivers of the glacier mass balance between the Karakoram and central Himalaya. Front. Earth Sci. 7, 107.

Braithwaite, R.J., Raper, S.C.B., 2009. Estimating equilibrium-line altitude (ELA) from glacier inventory data. Ann. Glaciol. 50, 127–132.

Brun, F., Berthier, E., Wagnon, P., et al., 2017. A spatially resolved estimate of High Mountain Asia glacier mass balances from 2000 to 2016. Nat. Geosci. 10 https://doi.org/10.1038/NGEO2999.

Cao, M.S., 1998. Detection of abrupt changes in glacier mass balance in the Tien Shan Mountains. J. Glaciol. 44 (147), 352–358.

Che, Y., Zhang, M., Li, Z., et al., 2017. Glacier mass-balance and length variation observed in China during the periods 1959–2015 and 1930–2014. Quat. Int. 454, 68–84.

Che, Y., Zhang, M., Li, Z., et al., 2018. Quantitative evaluation of glacier change and its response to climate change in the Chinese Tien Shan. Cold Reg. Sci. Technol. 153, 144–155.

Che, Y., Wang, S., Yi, S., et al., 2020a. Summer Mass Balance and Surface Velocity Derived by Unmanned Aerial Vehicle on Debris-Covered Region of Baishui River Glacier No. 1, Yulong Snow Mountain. Remote Sens. 12 (20), 3280.

Che, Y., Zhang, M., Li, Z., et al., 2020b. Understanding the mass balance characteristics of Qingbingtan Glacier No. 72 during the period of 2008-2014. J. Glaciol. Geocryol. 42, 318–331 (In Chinese).

Chen, J., Ohmura, A., 1990. Estimation of alpine glacier water resources and their change since the 1870s. IAHS Publ. 193, 127–135.

Chen, Y., Li, Z., Fan, Y., et al., 2015. Progress and prospects of climate change impacts on hydrology in the arid region of northwest China. Environ. Res. 139, 11–19.

Chen, Y., Li, W., Deng, H., et al., 2016. Changes in central Asia's water tower: past, present and future. Sci. Rep. 6, 35458.

Copland, L., Sylvestre, T., Bishop, M., et al., 2011. Expanded and recently increased glacier surging in the Karakoram. Arct. Antarct. Alp. Res. 43 (4), 503–516.

De Kok, R.J., Kraaijenbrink, P.D., Tuinenburg, O.A., et al., 2020. Towards understanding the pattern of glacier mass balances in High Mountain Asia using regional climatic modelling. Cryosphere 14 (9), 3215–3234.

Di Mauro, B., 2020. A darker cryosphere in a warming world. Nat. Clim. Chang. 10 (11), 979–980.

Ding, Y., Liu, S., Li, J., et al., 2006. The retreat of glaciers in response to recent climate warming in western China. Ann. Glaciol. 43, 97–105.
Ding, B., Yang, K., Qin, J., et al., 2014. The dependence of precipitation types on surface elevation and meteorological conditions and its parameterization. J. Hydrol. 513, 154–163.
Ding, B., Yang, K., Yang, W., et al., 2017. Development of a Water and Enthalpy Budget-based Glacier mass balance Model (WEB-GM) and its preliminary validation. Water Resour. Res. 53, 3146–3178.
Ding, Y.J., Zhang, S.Q., Zhao, L., et al., 2019. Global warming weakening the inherent stability of glaciers and permafrost. Sci. Bull. 64, 245–253.
Du, J.K., Xin, H.J., He, Y.Q., et al., 2013. Response of modern monsoon temperate glacier to climate change in yulong mountain. Sci. Geogr. Sin. 33 (7), 890–896 (In Chinese).
Dumont, M., Gardelle, J., Sirguey, P., et al., 2012. Linking glacier annual mass balance and glacier albedo retrieved from MODIS data. Cryosphere 6, 1527–1539.
Farinotti, D., Longuevergne, L., Moholdt, G., et al., 2015. Substantial glacier mass loss in the Tien Shan over the past 50 years. Nat. Geosci. 8, 716–722.
Farinotti, D., Immerzeel, W.W., de Kok, R.J., et al., 2020. Manifestations and mechanisms of the Karakoram glacier Anomaly. Nat. Geosci. 13 (1), 8–16.
Flanner, M.G., Shell, K.M., Barlage, M., et al., 2011. Radiative forcing and albedo feedback from the Northern Hemisphere cryosphere between 1979 and 2008. Nat. Geosci. 4 (3), 151–155.
Guo, W., Liu, S., Xu, J., et al., 2015. The second Chinese glacier inventory: data, methods and results. J. Glaciol. 61, 357–372.
Guo, D.L., Sun, J.Q., Yu, E.T., 2018. Evaluation of CORDEX regional climate models in simulating temperature and precipitation over the Tibetan Plateau. Atmos. Oceanic Sci. Lett. 11, 219–227.
Haeberli, W., Weingartner, R., 2020. In full transition: Key impacts of vanishing mountain ice on water-security at local to global scales. Water Security 11, 100074.
Hewitt, K., 2005. The Karakoram anomaly? Glacier expantion and the 'Elevation effect,' Karakoram Himalaya. Mt. Res. Dev. 25, 332–340.
Hock, R., 2005. Glacier melt: a review of processes and their modelling. Prog. Phys. Geogr. Earth Environ. 29, 362–391.
Hoelzle, M., Haeberli, W., Dischl, M., et al., 2003. Secular glacier mass balances derived from cumulative glacier length changes. Glob. Planet. Chang. 36, 295–306.
Huss, M., Farinotti, D., 2012. Distributed ice thickness and volume of all glaciers around the globe. J. Geophys. Res. Earth Surf. 117.
Huss, M., Hock, R., 2018. Global-scale hydrological response to future glacier mass loss. Nature Climate Change 8.
Huss, M., Sold, L., Hoelzle, M., et al., 2013. Towards remote monitoring of sub-seasonal glacier mass balance. Ann. Glaciol. 54, 75–83.
Immerzeel, W.W., van Beek, L.P.H., et al., 2010. Climate change will affect the asian water towers. Science 328, 1382–1385.
IPCC, 2013. Climate Change 2013: The Physical Science Basis. Contribution of Working Group I to the Fifth Assessment Report of the Intergovernmental Panel on Climate Change. Cambridge University Press, Cambridge, United Kingdom and New York, NY, USA.
IPCC, 2019. Special Report on the Ocean and Cryosphere in a Changing Climate. Cambridge University Press, Cambridge.
IPCC, 2021. Climate Change 2021: The Physical Science Basis. Contribution of Working Group I to the Six Assessment Report of the Intergovernmental Panel on Climate Change. Cambridge University Press, Cambridge, United Kingdom and New York, NY, USA.
Juen, M., Mayer, C., Lambrecht, A., et al., 2014. Impact of varying debris cover thickness on ablation: a case study for Koxkar Glacier in the Tien Shan. Cryosphere 8, 377–386.
Kääb, A., Berthier, E., Nuth, C., et al., 2012. Contrasting patterns of early twenty-first-century glacier mass change in the Himalayas. Nature 488 (7412), 495–498.
Kääb, A., Treichler, D., Nuth, C., et al., 2015. Brief communication: contending estimates of 2003–2008 glacier mass balance over the Pamir–Karakoram–Himalaya. Cryosphere 9, 557–564.
Kang, S., Zhang, Y., Qian, Y., et al., 2020. A review of black carbon in snow and ice and its impact on the cryosphere. Earth Sci. Rev. 210, 103346.
Kargel, J.S., Leonard, G.J., Bishop, M.P., et al., 2014. Global Land Ice Measurements from Space. Springer, Berlin Heidelberg.
Ke, L., Ding, X., Song, C., 2015. Heterogeneous changes of glaciers over the western Kunlun Mountains based on ICESat and Landsat-8 derived glacier inventory. Remote Sens. Environ. 168, 13–23.
Kendall, M.G., 1948. Rank Correlation Methods. Griffin, London.
Kraaijenbrink, P.D.A., Bierkens, M.F.P., Lutz, A.F., et al., 2017. Impact of a global temperature rise of 1.5 degrees Celsius on Asia's glaciers. Nature 549 (7671), 257–260.
Kumar, V., Shukla, T., Mishra, A., et al., 2020. Chronology and climate sensitivity of the post-LGM glaciation in the Dunagiri valley, Dhauliganga basin, Central Himalaya, India. Boreas 49 (3), 594–614.
Li, X., Cheng, G., Jin, H., et al., 2008. Cryospheric change in China. Glob. Planet. Chang. 62, 210–218.
Li, Z., Li, H., Chen, Y., 2011. Mechanisms and simulation of accelerated shrinkage of continental glaciers: a case study of Urumqi Glacier no. 1 in eastern Tianshan, Central Asia. J. Earth Sci. 22, 423–430.
Li, L., Yao, X., Liu, S., et al., 2019a. Glacier changes along the Silk Road Economic Belt in China in the past 50 years:Based on the revised First and Second Chinese Glacier Inventory. J. Nat. Resour. 34, 1506–1520 (In Chinese).
Li, S., Yao, T., Yu, W., et al., 2019b. Energy and mass balance characteristics of the Guliya ice cap in the West Kunlun Mountains, Tibetan Plateau. Cold Reg. Sci. Technol. 159, 71–85.
Li, Y., Ding, Y., Shangguan, D., et al., 2019c. Regional differences in global glacier retreat from 1980 to 2015. Adv. Clim. Chang. Res. 10, 203–213.
Liu, S., Ding, Y., Shangguan, D., et al., 2006. Glacier retreat as a result of climate warming and increased precipitation in the Tarim river basin, Northwest China. Ann. Glaciol. 43, 91–96.
Liu, S., Yao, X., Guo, W., et al., 2015. The contemporary glaciers in China based on the second Chinese Glacier Inventory. Acta Geograph. Sin. 70, 3–16 (In Chinese).
Mann, H.B., 1945. Nonparametric Tests against Trend. Econometrica 13, 245–259.
Mehta, M., Dobhal, D.P., Pratap, B., et al., 2014. Late quaternary glacial advances in the tons river valley, Garhwal Himalaya, India and regional synchronicity. The Holocene 24 (10), 1336–1350.
Mehta, M., Kumar, V., Garg, S., et al., 2021. Little Ice Age glacier extent and temporal changes in annual mass balance (2016-2019) of Pensilungpa Glacier, Zanskar Himalaya. Reg. Environ. Chang. 21 (38), 1–18.
Milner, A.M., Khamis, K., Battin, T.J., et al., 2017. Glacier shrinkage driving global changes in downstream systems. Proc. Natl. Acad. Sci. U. S. A. 114, 9770–9778.
Muhammad, S., Tian, L., Ali, S., et al., 2020. Thin debris layers do not enhance glaciers melt in the Karakoram. Sci. Total Environ. 141119.
Müller, F., Caflisch, T., Müller, G., 1977. Instructions for Compilation and Assemblage of Data for a World Glacier Inventory. In: Temporal Technical Secretariat for the World Glacier Inventory (TTS/WGI/IAHS(ICSI)/UNESCO), ETH Zürich 2007-12-19 1977..
Nesje, A., 1992. Topographical effects on the equilibrium-line altitude on glaciers. GeoJournal 27, 383–391.
Nie, Y., Pritchard, H.D., Liu, Q., et al., 2021. Glacial change and hydrological implications in the Himalaya and Karakoram. Nat. Rev. Earth Environ. https://doi.org/10.1038/s43017-020-00124-w.
Oerlemans, J., 2005. Extracting a climate Signal from 169 Glacier Records. Science 308, 675.
Osipov, E.Y., 2004. Equilibrium-line altitudes on reconstructed LGM glaciers of the northwest Barguzinsky Ridge, Northern Baikal, Russia. Palaeogeogr. Palaeoclimatol. Palaeoecol. 209, 219–226.
Östrem, G., 1959. Ice Melting under a Thin Layer of Moraine, and the Existence of Ice Cores in Moraine Ridges. Geogr. Ann. 41, 228–230.
Panagiotopoulos, F., Shahgedanova, M., Hannachi, A., et al., 2005. Observed trends and teleconnections of the Siberian high: a recently declining center of action. J. Clim. 18 (9), 1411–1422.
Paul, F., Bolch, T., Kääb, A., et al., 2015. The glaciers climate change initiative: Methods for creating glacier area, elevation change and velocity products. Remote Sens. Environ. 162, 408–426.
Pfeffer, W.T., Arendt, A.A., Bliss, A., et al., 2014. The Randolph Glacier Inventory: a globally complete inventory of glaciers. J. Glaciol. 60, 537–552.
Pritchard, H.D., 2019. Asia's shrinking glaciers protect large populations from drought stress. Nature 569, 649–654.
Qin, D.H., Ding, Y.J., Xiao, C.D., et al., 2018. Cryospheric Science: research framework and disciplinary system. Natl. Sci. Rev. 5, 255–268.
Radić, V., Hock, R., 2010. Regional and global volumes of glaciers derived from statistical upscaling of glacier inventory data. J. Geophys. Res. Earth Surf. 115.
Sen, P.K., 1968. Estimates of the Regression Coefficient based on Kendall's Tau. J. Am. Stat. Assoc. 63, 1379–1389.
Shean, D.E., Bhushan, S., Montesano, P.M., et al., 2020. A Systematic, Regional Assessment of High Mountain Asia Glacier Mass Balance. Front. Earth Sci. 7, 363.
Shi, Y., Liu, C., Kang, E., 2009. The Glacier Inventory of China. Ann. Glaciol. 50, 1–4.
Shukla, T., Mehta, M., Jaiswal, M.K., et al., 2018. Late Quaternary glaciation history of monsoon dominated Dingad basin, central Himalaya, India. Quat. Sci. Rev. 181, 43–64.
Su, B., Li, Z., Zhang, M., et al., 2015. A comparative study on mass balance between the continental glaciers and the temperate glaciers: taking the typical glaciers in the Tianshan Mountains and the Alps as examples. J. Glaciol. Geocryol. 37, 1131–1140 (In Chinese).
Su, B., Xiao, C., Chen, D., et al., 2019. Cryosphere services and human well-being. Sustainability 11.
Su, B., Xiao, C., Chen, D., et al., 2022. Mismatch between the population and meltwater changes creates opportunities and risks for global glacier-fed basins. Sci. Bull. 67, 9–12.
Sun, M., Liu, S., Yao, X., et al., 2015. Glacier changes in the Qilian Mountains in the past half century: based on the revised first and second Chinese Glacier Inventory. Acta Geograph. Sin. 70, 1402–1414 (In Chinese).
Tamang, S.K., Ebtehaj, A.M., Prein, A.F., et al., 2019. Linking Global changes of Snowfall and Wet-Bulb Temperature. J. Clim. 39–59.
Tian, H., Yang, T., Liu, Q., 2014. Climate change and glacier area shrinkage in the Qilian mountains, China, from 1956 to 2010. Ann. Glaciol. 55, 187–197.
Tian, H.Z., Yang, T.Z., Lv, H., et al., 2016. Climate change and glacier area variations in China during the past half century. J. Mt. Sci. 13, 1345–1357.
Wang, Y., Hou, S., Huai, B., et al., 2018. Glacier anomaly over the western Kunlun Mountains, Northwestern Tibetan Plateau, since the 1970s. J. Glaciol. 64 (246), 624–636.
Wang, P., Li, Z., Li, H., et al., 2020a. Glaciers in Xinjiang, China: past changes and Current Status. Water 12, 2367.
Wang, S., Che, Y., Pang, H., et al., 2020b. Accelerated changes of glaciers in the Yulong Snow Mountain, Southeast Qinghai-Tibetan Plateau. Reg. Environ. Chang. 20, 38.
Wang, X., Chen, D., Pang, G., et al., 2020c. A climatology of surface–air temperature difference over the Tibetan Plateau: results from multi-source reanalyses. Int. J. Climatol. 40 (14), 6080–6094.
Wester, P., Mishra, A., Mukherji, A., et al., 2019. The Hindu Kush Himalaya Assessment: Mountains, Climate Change, Sustainability and People. Springer, Switzerland.

WGMS, 2020. Fluctuations of Glaciers Database. World Glacier Monitoring Service, Zurich, Switzerland.
Wu, J., Gao, X., 2013. A gridded daily observation dataset over China region and comparison with the other datasets. Chin. J. Geophys. 56, 1102–1111.
Wu, L., Li, X., 2011. Data quality evaluation for database of the first Chinese glacier inventory. In: International Conference on Remote Sensing, Environment and Transportation Engineering, pp. 2067–2070. https://doi.org/10.1109/RSETE.2011.5964712. (in Chinese with English abstract).
Wu, K., Liu, S., Jiang, Z., et al., 2018. Recent glacier mass balance and area changes in the Kangri Karpo Mountains from DEMs and glacier inventories. Cryosphere 12, 103–121.
Xiang, L., Wang, H., Jiang, L., et al., 2021. Glacier mass balance in High Mountain Asia inferred from a GRACE release-6 gravity solution for the period 2002–2016. J. Arid Land 13 (3), 224–238.
Xiao, C., Liu, S., Zhao, L., et al., 2007. Observed changes of cryosphere in China over the second half of the 20th century: an overview. Ann. Glaciol. 46, 382–390.
Xiao, C., Li, Z., Zhao, L., et al., 2012. High Asia cryospheric observatiom a proposed network under Global Cryosphere Watch GDV. Sci. Cold Arid Regions 4, 1–12.
Xin, W., Li, Z., Zhang, H., et al., 2017. Spatial-temporal variation of glacier resources in Chinese Tianshan Mountains since 1959. Acta Geograph. Sin. 72, 1594–1605 (In Chinese).
Xu, C., Li, Z., Li, H., et al., 2019. Long-range terrestrial laser scanning measurements of annual and intra-annual mass balances for Urumqi Glacier No. 1, eastern Tien Shan, China. The Cryosphere 13, 2361–2383.
Yang, M., Wang, X., Pang, G., et al., 2019. The Tibetan Plateau cryosphere: Observations and model simulations for current status and recent changes. Earth Sci. Rev. 190, 353–369.
Yao, T., Wang, Y., Liu, S., et al., 2004. Recent glacial retreat in High Asia in China and its impact on water resource in Northwest China. Sci. China Ser. D Earth Sci. 47, 1065–1075.
Yao, T., Thompson, L., Yang, W., et al., 2012a. Different glacier status with atmospheric circulations in Tibetan Plateau and surroundings. Nat. Clim. Chang. 2, 663–667.
Yao, X., Liu, S., Guo, W., et al., 2012b. Glacier Change of Altay Mountain in China from 1960 to 2009 -Based on the Second Glacier Inventory of China. J. Nat. Resour. 1734–1745 (In Chinese).
Yao, T., Xue, Y., Chen, D., et al., 2019. Recent third pole's rapid warming accompanies cryospheric melt and water cycle intensification and interactions between monsoon and environment: Multidisciplinary approach with observations, modeling, and analysis. Bull. Am. Meteorol. Soc. 100 (3), 423–444.
Zemp, M., Hoelzle, M., Haeberli, W., 2009. Six decades of glacier mass-balance observations: a review of the worldwide monitoring network. Ann. Glaciol. 50, 101–111.
Zemp, M., Thibert, E., Huss, M., et al., 2013. Reanalysing glacier mass balance measurement series. Cryosphere 7, 1227–1245.
Zemp, M., Frey, H., Gärtner-Roer, I., et al., 2015. Historically unprecedented global glacier decline in the early 21st century. J. Glaciol. 61, 745–762.
Zemp, M., Huss, M., Thibert, E., et al., 2019. Global glacier mass changes and their contributions to sea-level rise from 1961 to 2016. Nature 568 (7752), 382–386.
Zhang, M., Wang, S., Li, Z., et al., 2011. Variation of glacier area in China against the warming in the past 50 years. Acta Geograph. Sin. 66, 1155–1165.
Zhang, G., Yao, T., Xie, H., et al., 2020. Response of Tibetan Plateau lakes to climate change: Trends, patterns, and mechanisms. Earth Sci. Rev. 208, 103269.
Zhang, Y., Gao, T., Kang, S., et al., 2021. Albedo reduction as an important driver for glacier melting in Tibetan Plateau and its surrounding areas. Earth Sci. Rev. 103735.
Zhou, Z., Han, N., Liu, J., et al., 2020. Glacier variations and their response to climate change in an arid inland river basin of Northwest China. J. Arid Land 12, 357–373.
Zhu, M., Yao, T., Yang, W., et al., 2018a. Differences in mass balance behavior for three glaciers from different climatic regions on the Tibetan Plateau. Clim. Dyn. 50, 3457–3484.
Zhu, M., Yao, T., Yang, W., et al., 2018b. Reconstruction of the mass balance of Muztag Ata No. 15 glacier, eastern Pamir, and its climatic drivers. J. Glaciol. 64 (244), 259–274.